Discovery and Pharmacological Study of Drug Candidate Agents for the Treatment of Inflammatory Diseases

January 2019

Hisashi WAKITA

Discovery and Pharmacological Study of Drug Candidate Agents for the Treatment of Inflammatory Diseases

A Dissertation Submitted to
the Graduate School of Life and Environmental Sciences,
the University of Tsukuba
in Partial Fulfillment of the Requirements
for the Degree of Doctor of Philosophy in Biotechnology
(Doctoral Program in Bioindustrial Sciences)

Hisashi WAKITA

Table of Contents

Abbreviation

ANOVA	analysis of variance
cAMP	cyclic adenosine monophosphate
CCR	CC chemokine receptor
CHO	Chinese hamster ovary
CX3CR1	CX3C chemokine receptor 1
DRG	dorsal root ganglion
EC_{50}	half maximal (50%) effective concentration
EDTA	ethylenediaminetetraacetic acid
EGTA	ethylene glycol tetraacetic acid
GPCR	G protein-coupled receptor
[^{35}S]GTPγS	guanosine 5'-*O*-(3-[^{35}S]thio)triphosphate
HEPES	4-(2-hydroxyethyl)-1-piperazineethanesulfonic acid
IBD	inflammatory bowel disease
IC_{50}	half maximal (50%) inhibitory concentration
IFN	interferon
Ig	immunoglobulin
IL	interleukin
LSD	least significant difference
MCP-1	monocyte chemoattractant protein-1
MFI	mean fluorescence intensity
NK cell	natural killer cell
PBS	phosphate-buffered saline
PDE	phosphodiesterase

PVT	polyvinyltoluene
QOL	quality of life
RLU	relative light units
SAR	structure-activity relationship
SCID	severe combined immunodeficiency
Th	T-helper
TNF	tumor necrosis factor
TRPV1	transient receptor potential vanilloid 1
WGA	wheat germ agglutinin

Chapter 1. Preface

The mission of the pharmaceutical industries is to contribute to the improvement of welfare of people in the world by developing and supplying an excellent medicine. The medicines show the effect by changing the intercellular or intracellular transmission. Most of drug targets are proteins from the view point of molecular biology. According to literature that researched the drug targets in 1996, cell membrane receptors including GPCR (G protein-coupled receptor) constitute the largest subgroup with 45% of all targets, and enzymes account for 28% of all researched drug targets [1].

The basis in a modern drug development process was a process that had been used to select the antibiotic drugs. The drug development was able to be advanced with a simple method due to clear drug target such as pathogen microorganism. Cimetidine, histamine type 2 receptor antagonist, was discovered by J. Black in 1950's, and the medicine is widely used for the treatment of acid-peptic disease and heartburn. The basic model in the research and development process of a modern drug development completed this time. The process is shown in Fig. 1-1 [2].

The processes from finding of hit compounds to optimization of lead compounds are called drug discovery as screening step of drug candidates. First of all, it is necessary to construct the screening system in the process. It is the first stage where the compound judges whether there is a possibility as a medicine. The originality of the screening system is a key to find the candidate compound. In a case of no information on compound structure to find the medicine, the compounds are screened at random and the hit compounds are selected based on pharmacological activity and tractability of compound synthesis. The group of compounds used at random is called the compound

library, and hit rate in the screening depends on diversity of compound scaffold not the number of compounds at the library. Common chemical structure in the hit compounds, which have pharmacological activity, indicates a series of structural aspect which is recognized to drug target molecule. It is a little that a perfect lead compound appears in a short-term screening. Medicinal chemists change the side chain of the hit compounds based on investigation of relationship between the compound structure and activity, and select the lead compounds by improving the pharmacological effect. To select the candidate compound with potent pharmacological activity and few side effects, the medicinal chemists perform compound optimization by more detail modification of the lead compound. In the process, originality and high technology of the medicinal chemists are required, and two or more evaluation systems are additionally utilized including *in vitro* assay systems and *in vivo* disease model systems.

To decide the molecule of drug target, it is necessary to decide the disease as the drug indication. The item considered to decide the disease is as follows: robust relationship between drug target and disease, trends of the diseases and patients, necessity on clinical site, differentiation with in existence drug, assumed sales and profit. According to the disease investigation, two drug discovery projects were undertaken to create novel anti-inflammatory drugs for the treatment of atopic dermatitis and IBD (inflammatory bowel disease). The drug targets were decided to PDE4 and CX3CR1 for atopic dermatitis and IBD, respectively.

To find candidate compounds in the two drug discovery programs, compound screening system, *in vitro* assay system and *in vivo* disease model were established (Table 1-1) [3 – 6]. In the project to find compound that show blockage of CX3CR1 pathway, GPCR-focused library was utilized as screening library according to the

feature of the target molecule. Identification of candidate compounds, E6005 and E6130, was achieved by utilization of the compound evaluation system and contribution of medicinal chemists.

To investigate whether it is worth that the candidate compounds introduce clinical, pharmacological study of these compound was performed and described in this dissertation.

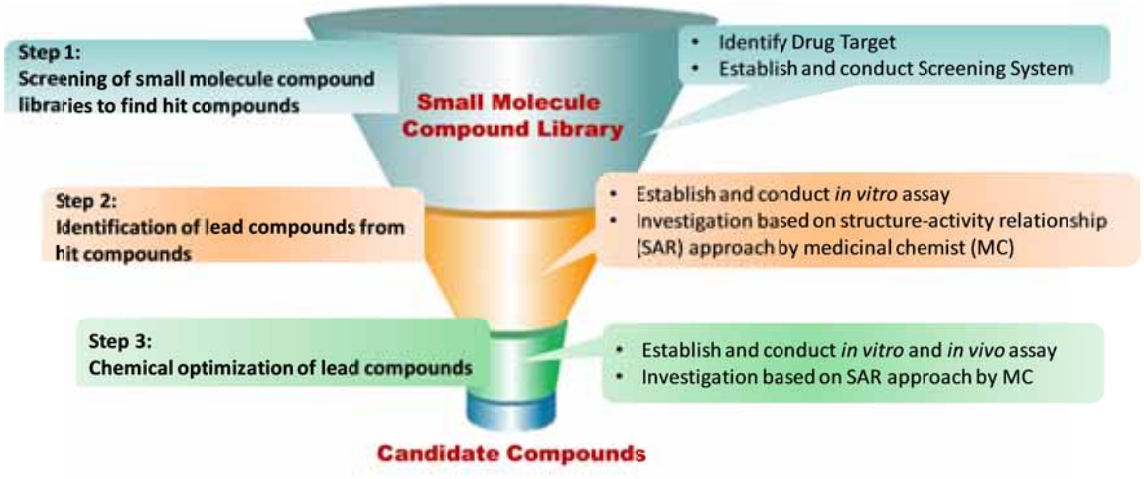

Fig. 1-1 Flow of drug discovery.

Table 1-1. *In vitro* and *in vivo* assays to find candidate compounds

	E6005	**E6130**
Screening compounds	Small molecule compound library (created by Eisai)	
Screening assay	PDE4 enzyme assay	Fluorescent microvolume assay (Receptor binding assay)
In vitro assay	TNF-α production assay	Fractalkine-induced chemotaxis assay
In vivo assay	Oxazolone-induced atopic dermatis model	$CD4^{+}CD45Rb^{high}$T cell-transferred colitis model

Chapter 2. Mechanism elucidation of anti-pruritic effect of selective PDE4 inhibitor E6005 as a therapeutic agent of atopic dermatitis

2.1. Introduction

Atopic dermatitis is a chronic inflammatory skin disease associated with pruritus. In cases of chronic atopic dermatitis lesions, pruriceptive neurons are sensitized by inflammatory mediators to respond more intensely and at a lower threshold to pruritogenic stimulation [7, 8], intensifying the itch and contributing to the chronic nature of the lesion [9]. Chronic pruritus is poorly managed by current treatment approaches such as antihistamines and topically applied steroids. The inadequacy of current conventional antipruritic therapy necessitates the development of new agents with novel mechanisms of action.

According to an epidemiological survey by the International Study of Asthma and Allergies in Childhood (ISAAC), the prevalence of atopic dermatitis is 7.3% at ages 6 to 7 (prevalence in regional surveys ranged from 1.1% to 18.4%; 16.9% in Japan); and 7.4% at ages 13 to 14 (prevalence in regional surveys: 0.8% to 17.7%; 10.5% in Japan). Prevalence tended to be high in Oceania, Northern Europe, and industrially advanced countries, and lower in developing countries such as Asia and Eastern Europe [10, 11]. The following prevalences were reported in adults in Japan and the U.S., respectively: adults in their 20's: 9.8%, 18%; 30's: 3.5% to 8.7%, 13%; 40's: 3.1% to 4.4%, 10%; and 50's-60's: 2.6%, 4% to 6% [12 – 14]. Prevalence thus tends to decrease with age.

Atopic dermatitis is a subtype of eczema/dermatitis, and infiltration of

inflammatory cells, including lymphocytes, eosinophils, and mast cells are present in eczema lesions [15, 16]. Leukocyte infiltration into skin lesions is caused by chemokines, which are produced in the epidermal keratinocyte [17], and in particular, the level of the Th2 chemokine, thymus and activation-regulated chemokine (TARC)/CCL17 is correlated with the severity of atopic dermatitis [18]. Antigen-presenting cells and mast cells in the skin are involved in inflammatory reactions by presenting antigens or releasing histamines and cytokines through the engagement of allergen-specific IgE antibodies to high-affinity IgE receptors. In the acute stage, IL-4, 5, 9, 10, and 13 are produced from Th2 cells, and in the chronic stage, IFN-γ and IL-2 are produced from Th1 cells, which aggravate the disease and cause chronicity. These inflammatory reactions can also be induced by environmental factors such as bacterial infections [19].

Cyclic AMP (cAMP) is an intracellular signal molecule which modulates various cellular responses. Intracellular cAMP levels, which are regulated by a balance between production by adenylate cyclase and degradation by phosphodiesterase (PDE), modulate a signal transduction cascade leading to cellular response. There are several PDE isozymes. PDE4 is a major isozyme involved in the inflammatory reaction, which plays an important role in the activation of inflammatory cells including T cells and monocytes [20, 21]. The exaggerated response of inflammatory cells leads to various diseases. In atopic dermatitis, increased PDE activation in monocytes is thought to be involved in pathogenesis, through the induction of an abnormal inflammatory response [22]. Monocytes in patients have decreased levels of cAMP, due to increased PDE activity, which promotes the production of prostaglandin E2 and IL-10. This results in an increase of IL-4, but a decrease of IFN-γ production in T-cells and subsequent

activation of Th2 cells, and eventually causes the development of the disease.

Atopic dermatitis is accompanied by dry skin due to abnormalities in the physiological function of the skin, and reduced moisture from abnormal barrier function [23]. On the other hand, the intense itching associated with atopic dermatitis induces scratching, which leads to secondary inflammatory skin lesions [24]. This intense itching results from itch hyper-sensitivity caused by lowering of the response threshold of peripheral nerves to pruritogens including histamine [7, 25], the sprouting of nerve endings [26], and the spontaneous activity of itchy C-fibers [27 – 29].

Currently, there is no drug treatment that completely cures atopic dermatitis [30, 31]. Topical steroids are the first-line treatment for atopic inflammation, and the appropriate potency is selected based on both the severity and location of the rash and the age of the patient. Tacrolimus ointment, a calcineurin inhibitor, is indicated for use when topical steroids are not sufficiently effective or when adverse drug reactions are a concern. UV phototherapy and oral cyclosporine can be administered in the most severe cases. In addition, skin care with moisturizing and protective agents is recommended for treating abnormalities in the physiological function of the skin. There are often specific aggravating factors in the daily life of the patient. The identification and subsequent elimination of these factors, as well providing lifestyle guidance to the patient should be considered. On the other hand, antihistamines and anti-allergy drugs are also used to prevent itching and aggravation of symptoms from scratching. However, they have a poor effect on pruritogens other than histamine [7, 25]. These oral medications should be considered as an adjuvant to topical therapy. Even under the current therapeutic system, the disturbance of sleep due to itching is significant, which has a major impact not only on the patient's QOL, but also on the QOL of the patient's family [32].

In the pathogenesis of atopic dermatitis, an itch-scratch-inflammation cycle is established. As a result of interactions between itching and inflammation, skin lesions become aggravated and chronic. Currently, there are no effective drugs for itching, and a drug which is demonstrated to be effective for both itching and inflammation would have the potential to become a promising new therapeutic agent. Ishii *et al.* reported that the PDE4 inhibitor, E6005 showed an immediate anti-pruritic effect as well as an anti-inflammatory effect with suppressed cytokine expression [33] (Figs. 2-1 – 2-3, Table 2-1). However, the mechanism underlying the immediate anti-pruritic effect of E6005 remains unknown.

In this chapter, I describe the anti-pruritic effect of E6005 in an itch model and evaluate a putative mechanism of pruritus inhibition. My study demonstrated that E6005 suppressed pruritus by inhibiting C-fiber nerve depolarization evoked by TRPV1 activation, through modulation of cAMP signaling. Itch is a major manifestation in a number of skin disorders, including atopic dermatitis. E6005 holds promise as a novel anti-itch therapy.

2.2. Materials and Methods

2.2.1. Test compound and reagents

E6005 [6], roflumilast and JNJ17203212 were synthesized in-house at Eisai Co., Ltd. Chemical structures of E6005 and roflumilast are shown in Figs. 2-4 and 2-5, respectively. Vaseline-based E6005 ointment was prepared in-house at Eisai Co., Ltd. Oxazolone, forskolin, betamethasone, naltrexone hydrochloride, capsaicin, collagenase type IV, amitriptyline, bupivacaine, and lidocaine were purchased from Sigma-Aldrich (St. Louis, MO, USA). Terfenadine was purchased from Kanto Chemicals Co., Inc. (Tokyo, Japan). FK506 (tacrolimus) was purchased from Wako Pure Chemical Industries Ltd. (Osaka, Japan). Rat β-NGF was purchased from R&D Systems Inc. (Minneapolis, MN, USA).

2.2.2. Animals

Male HR-1 mice (5 weeks old) and male Wistar rats (5 weeks old) were purchased from Hoshino Experimental Animal Supply (Saitama, Japan) and Charles River Laboratories Japan, Inc. (Kanagawa, Japan), respectively. All animals were kept in a pathogen-free animal facility with temperature maintained at 20–26°C, humidity 40–70%, and a 12-h day/night cycle, with access to food and water *ad libitum*. All procedures were performed at the animal facility accredited by the Center for Accreditation of Laboratory Animal Care and Use, Japan Health Sciences Foundation.

All protocols were approved by the Institutional Animal Care and Use Committee and carried out according to Eisai Animal Experimentation Regulations.

2.2.3. Isolation of dorsal root ganglion (DRG) neurons

Primary dorsal root ganglion (DRG) neurons were isolated as previously described with slight modifications [34]. Briefly, isolated DRG from adult Wister rats were collected in cold Hank's balanced salt solution (HBSS), centrifuged, and then re-suspended in F-12 nutrient mixture containing collagenase (2 mg/mL) and fetal calf serum (FCS, 10%). After 90 min of incubation at 37°C with agitation, the cells were spun down and treated with Trypsin-EDTA solution for 15 min at 37°C. The suspension of neurons was washed and suspended in Dulbecco's modification of Eagle's medium (DMEM) containing 10% FCS. Cultures were maintained for 2-4 days in a humidified atmosphere (37°C, 5%CO_2).

2.2.4. Electrophysiological recordings

Small-sized DRG neurons (diameter, <30 μm), which have been shown to exhibit high capsaicin sensitivity [35, 36], were selected for whole-cell patch clamp recording at room temperature (20-22°C) by using an Axopatch 1D amplifier (Axon Instruments, Union City, CA, USA). The micropipettes used had resistances of 2-6 MΩ. The standard pipette solution contained 4 mM ATP, 130 mM KCl, 2 mM $MgCl_2 \cdot 6H_2O$, 5 mM EGTA, 0.5 mM $CaCl_2$, and 10 mM HEPES, with pH adjusted to 7.2 by using NaOH. The standard external solution contained 130 mM NaCl, 5 mM KCl, 2 mM $MgCl_2 \cdot 6H_2O$, 2 mM $CaCl_2$, and 10 mM HEPES. The low-pass filter was set at 5 kHz. The cells were superfused with combinations of capsaicin with vehicle, E6005 (0.1 μM and 1 μM), roflumilast, betamethasone, or tacrolimus. All data acquisition and analysis were performed using pClamp 8.02 software (Axon Instruments, Sunnyvale, CA, USA). The capsaicin-evoked membrane depolarization (ΔmV) was calculated as the difference

between the membrane potential measured before and after the addition of capsaicin.

2.2.5. Nav1.2 current assay

hNav1.2-CHO cell line has been established in Eisai Tsukuba Labs. The cells were grown in DMEM+GlutaMAX^{TM} –I medium (10569, Gibco, Waltham, MA, USA) containing 5% FBS and Antibiotic-Antimycotic (15240, Gibco, Waltham, MA, USA). Two or 3 days before the automated patch clamp experiments using IonWorks-Quattro (Molecular Devices Corporations, San Jose, CA, USA), 1 or 0.5 x 10^6 cells was seeded into F225 culture flasks. After rinse by D-PBS(-) (045-29795, Wako, Osaka, Japan) and treatment by 0.05% trypsin-EGTA (25300, Gibco, Waltham, MA, USA), cells were collected and suspended into the external buffer at the density of 5.0 x 10^6 cells/mL. For the patch clamp experiments, the external buffer contained 138 mM NaCl, 2.7 mM KCl, 0.9 mM $CaCl_2$, 0.5 mM $MgCl_2$, 1.5 mM KH_2PO_4, and 8.1 mM Na_2HPO_4 and the internal buffer contained 100 mM K-gluconate, 40 mM KCl, 3.2 mM $MgCl_2$, 5 mM EGTA and 5 mM HEPES. Nav1.2 current was evoked by the application of train of 30 pulses to 0 mV from a holding potential of -70 mV at 20 Hz.

2.2.6. Oxazolone-induced pruritus model in HR-1 mice

Oxazolone-induced dermatitis was developed in HR-1 mice according to the method described in a previous report [38] with some modifications. Briefly, HR-1 mice were sensitized by painting 100 μL of 0.5% oxazolone dissolved in acetone/ethanol solution (1:1) onto the skin of the abdomen. Scratching was evoked by painting 10 μL of 1-1.5% oxazolone solution onto ear skin twice a week, starting from 6 days after sensitization. Scratching behavior was quantified using the MicroAct system

(Neuroscience, Inc., Tokyo, Japan). The instances of scratching behavior were counted for 90 min. Naltrexone hydrochloride was dissolved in saline and was subcutaneously administered 15 minutes before the 4th oxazolone challenge. Terfenadine was dissolved in saline and was orally administered 1 h before the 4th oxazolone challenge. Forskolin was dissolved in acetone/ethanol solution (1:1) and was topically administered 1 h before the 4th oxazolone challenge. JNJ17203212 was dissolved in polyethylene glycol 400 and was orally administered 1 h before the 4th oxazolone challenge. Vaseline-based E6005 ointment was administered topically 4-5 h before the 4th-6th challenge.

2.2.7. Statistical analysis

In all studies except electrophysiological study, the Student's *t*-test was used to analyze differences between two groups, and the Dunnett test was used for multiple comparisons among treatment groups. *P* values <0.05 were considered statistically significant.

In the electrophysiological study, data were analyzed using unpaired t-tests and one-way ANOVA followed by Dunnett's multiple comparison test by using the software package SAS ver. 6.12 (SAS Institute Japan, Ltd., Tokyo, Japan). A value of $p < 0.05$ (two-sided) was considered statistically significant.

2.3. Results

2.3.1. Effect of E6005 on capsaicin-evoked depolarization of dorsal root ganglion (DRG) neurons

The effect of E6005 on depolarization evoked by capsaicin, a TRPV1 agonist, was examined in the primary small-sized DRG neurons, which have been reported to be relevant to itch [35, 36]. Under current-clamp condition, 1 μM capsaicin elicited a typical change in membrane potential and action potential firing (Fig. 2-6a), which was attenuated by E6005 in a concentration-dependent manner (Fig. 2-6bc). Roflumilast, a structurally distinct PDE4 inhibitor, also decreased the capsaicin-evoked membrane potential change (Fig. 2-6c). Anti-inflammatory agents tacrolimus and steroid betamethasone did not significantly alter capsaicin-induced changes in membrane potential in this experimental setting (action potential firing rate of tacromilus: 2/4, betamethasone: 3/5). In contrast, forskolin, an agent that activates the cAMP signaling pathway, reduced the magnitude of depolarization (Fig. 2-6d).

2.3.2. Effects of E6005, naltrexone, terfenadine, forskolin and JNJ17203212 on oxazolone-induced scratching behavior in HR-1 mice

Oxazolone-induced dermatitis is characterized by severe mononuclear cell recruitment. This characteristic inflammatory skin damage means that oxazolone-dermatitis is a useful *in vivo* tool for pathogenic studies to select potential therapeutics for the treatment of inflammatory responses associated with the skin. A mouse model of chronic scratching was established by application of the chemical irritant oxazolone and used to assess the anti-pruritic effect of E6005. Oxazolone-sensitized mice were repeatedly challenged on the ear with re-application of

oxazolone to establish intermittent scratching responses upon irritations. Oxazolone challenge initially elicited a weak response with approximately 200 instances of scratching. The number of scratching instances increased with repeated application of oxazolone, reaching a plateau after the 3rd challenge (Fig. 2-7). The scratching behavior, as assessed at the 4th application of oxazolone, was resistant to histamine H_1-receptor antagonist terfenadine, but sensitive to an opioid receptor antagonist naltrexone (Fig. 2-8ab), reflecting the observations in atopic dermatitis patients [39]. E6005 ointment (0.01% and 0.03%, w/v) caused an immediate and significant reduction of scratching response in a dose-dependent manner at day 15. Furthermore, application of E6005 ointment at 3 or 4-day intervals attenuated the scratching at each oxazolone-challenge in a dose-dependent manner (Fig. 2-9). In order to evaluate the involvement of cAMP elevation on scratching behavior, the effect of adenylyl cyclase-activator forskolin was assessed. Forskolin application significantly decreased oxazolone-elicited scratching behavior with immediate effect, as assessed 15 days after sensitization (Fig. 2-10a).

To study the involvement of transient receptor potential vanilloid 1 (TRPV1) in the chronic itch model, the effect of TRPV1 antagonist JNJ17203212 was examined. Oral administration of 30 mg/kg JNJ17203212 significantly reduced oxazolone-elicited scratching (Fig. 2-10b).

2.3.3. Effect of E6005, amitriptyline, bupivacaine, and lidocaine on Na^+ current recorded in hNav1.2-CHO cells

Topical application of E6005 immediately inhibits itching behaviour as well as itch-related cutaneous nerve firing in a mouse model. Local anaesthetics such as Na^+-channel blockers have been used clinically for relief of pruritus. To verify whether

this effect is due to a local anaesthetic activity, effect of E6005 on Na^+ current recorded in hNav1.2-CHO cells was investigated. The Na^+-channel blockers amitriptyline, bupivacaine, and lidocaine inhibited Nav1.2 current in a concentration-dependent manner, with half-maximal inhibitory concentration (IC_{50}) values (μM) of 1.3, 3.3, and 86.3, respectively. E6005 did not show any inhibitory activity for Nav1.2 current at ≤20 μM (Fig. 2-11). In this experiment, the maximal attainable concentration of E6005 was 20 μM owing to its limited solubility.

2.4. Discussion

In chronic pruritic skin, C-fibers are rendered more responsive to pruritogenic stimulations by inflammatory mediators, resulting in intense and persistent itch response [7, 8]. In my chronic itch model, established by repeated stimulation with a chemical irritant, skin lesions showed typical symptoms of chronic pruritic skin, such as reddening and thickening [33]. Scratching behavior was observed to increase with the progression of inflammation, as seen in patients, reaching a reproducible scratch response to the skin irritant following repeated applications. Topically applied E6005 and cAMP-elevating agent forskolin suppressed the scratching behavior with immediate effect in this model, indicating that E6005 possessed therapeutic potential for management of chronic pruritus. Interestingly, the observed anti-pruritic effects preceded the improvement of inflammatory symptoms. Additionally, the inhibition of scratching by topical forskolin administration suggests that cAMP signaling plays a suppressive role in the process of itch generation, confirming previous findings by other laboratories [40].

TRPV1 played a role in the generation of itch in my chronic scratching model. Recent advances in neurophysiology of pruritus revealed that C-fibers can be categorized as two distinct nerve fiber types by size, with the smaller TRPV1-positive population playing a major role in the generation of itch [36, 41 – 43]. The population of smaller DRG nerve fibers was selected for the electrophysiological investigation. The DRG neurons studied showed rapid depolarization in response to the TRPV1 activator capsaicin, with increased membrane potential firings. Attenuation of capsaicin-induced membrane depolarization by two structurally different PDE4 inhibitors suggests that inhibition of PDE4 enzymes modulates C-fiber function. Additionally, cAMP elevator

forskolin diminished the capsaicin-induced depolarization, suggesting that the inhibition of membrane depolarization by E6005 may be mediated by alterations of cAMP signaling. These findings demonstrated that PDE4 inhibition could suppress DRG function by increasing intracellular cAMP levels, which contributes to the immediate anti-scratching mechanism. In contrast to the effects of E6005 and roflumilast, anti-inflammatory drugs betamethasone and tacrolimus did not significantly suppress nerve activation [33]. Since steroid administration did not inhibit the scratching behavior [33], the ability of tested compounds to suppress the TRPV1-mediated depolarization of DRG nerve fibers seemed to be reflected in their immediate anti-scratching effect *in vivo*. Tacrolimus is, however, reported to inhibit DRG activation by a longer pretreatment than my study [44]. The lack of the effect in my study may be due to the inadequate pre-incubation time. E6005 directly affected DRG neuron. But, the mode of action seems to unlike tacrolimus because E6005 exerted the suppressive effect without stimulating DRG. This was also confirmed by measuring C-fiber activity in animals with atopic dermatitis [45] and absence of burning in patients with atopic dermatitis [46]. Finally, my findings allow to rule out the possibility that the observed inhibition of scratching behavior of E6005 is due to local anesthetic activity because it did not inhibit the sodium channel responsible for local anesthesia (Fig. 2-8). The inhibitory effect of cAMP on depolarization was intriguing but was in contrast to that on pain, upon which it augments the sensitivity and magnitude. Han *et al.* reported that TRPV1-positive itch-specific DRG neurons that express the Mas-related G protein-coupled receptor (Mrgpr) generate itch but not pain upon capsaicin stimulation [43]. In addition, distinct mechanisms for intra-cellular signaling between itch and pain generation have been suggested [46]. In the present study, forskolin suppressed

depolarization, instead of augmenting it, and cutaneous cAMP elevation has been shown to decrease itching in a mouse model of chronic itch [45]. Therefore, a distinct cAMP-driven inhibitory signal might be present in itch-related DRG neurons. Further experiments to study the modification of intra-cellular molecules by cAMP as well as Mrgpr expression in the preparation of DRG neurons are required to confirm the effect of E6005 on DRG neurons.

As summary of this chapter, I show that E6005, which was identified *via* screening of Eisai's small molecule compound libraries and chemical optimization based on structure activity relationship approach, may provide a new approach to manage skin inflammation and pruritus in the treatment of atopic dermatitis. As a next step, to study whether the evaluation system of drug discovery is also suitable for other drug discovery program, screening system of the compound libraries was established to develop an anti-inflammatory drug through inhibition of CX3CR1 pathway for treatment of IBD. I show pre-clinical efficacy of E6130, which was identified from the screening and chemical optimization, as the drug of IBD in the next chapter.

Table 2-1. *In vitro* inhibitory effects of E6005 on cytokine release in lymphocyte and monocyte derived from human peripheral blood

Lymphocyte				Monocyte	
IL-2[a]	IL-4[a]	IFN-γ[b]	TNF-α[b]	IL-12[c]	TNF-α[c]
3.1	2.7	0.87	0.78	0.49	0.79
(2.0 - 4.9)	(0.90 - 8.3)	(0.015 - 52)	(0.38 - 1.6)	(0.21 - 1.2)	(0.085 - 7.4)

Data given as mean IC_{50} values (nM) calculated from concentration-inhibition curves from three different experiments; 95% confidence intervals are shown in parentheses.

[a]Anti-CD3/CD28 antibody-stimulated.

[b]Phytohemagglutinins-P-stimulated.

[c]Lipopolysaccharide-stimulated.

IFN-γ = interferon-γ, IL-2, -4, -12 = interleukin 2, -4, -12, TNF-α = tumor necrosis factor-α.

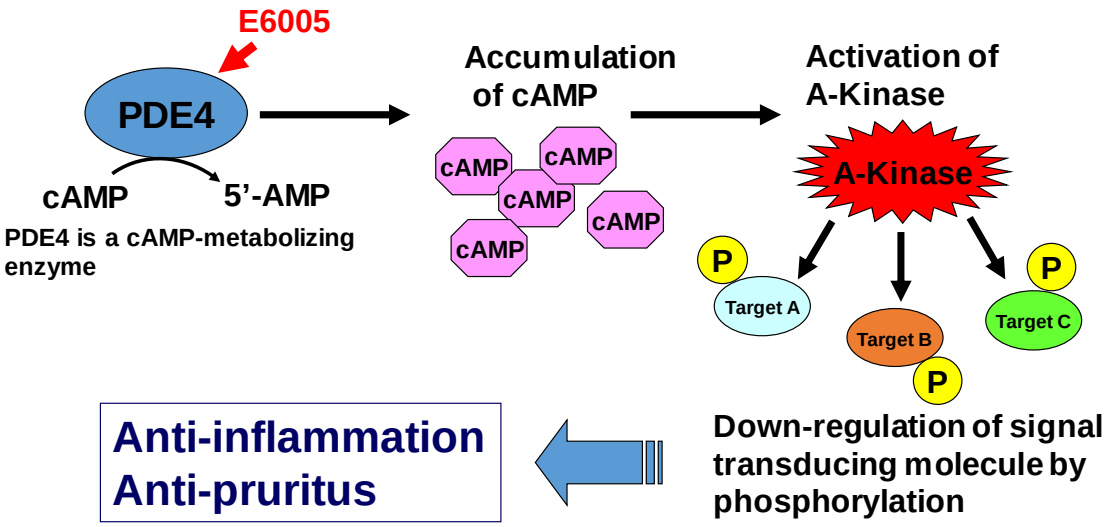

Fig. 2-1 Assumed mode of action of E6005.

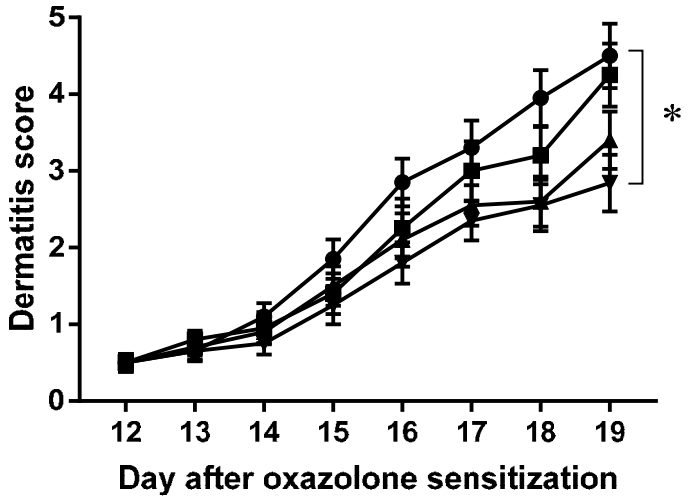

Fig. 2-2 Theraputic effect of topically applied E6005 on oxazolone-induced dermatitis score in NC/Nga mice.

15 μL of 0.003% E6005 ointment (solid squares), 0.01% E6005 ointment (solid triangles), 0.03% E6005 ointment (solid inverted triangles), or Vaseline based-vehicle ointment (solid circles) was administrated once a day from day 12 to day 18 onto the ears of NC/Nga mice that were sensitized and challenged with oxazolone. Skin lesion was scored according to the following symptoms: erythema/hemorrhage, excoriation, and oozing/crusting. Results are expressed as the mean ± S.E.M. (n = 19 or 20). * $P <$ 0.05 versus the vehicle-treated group.

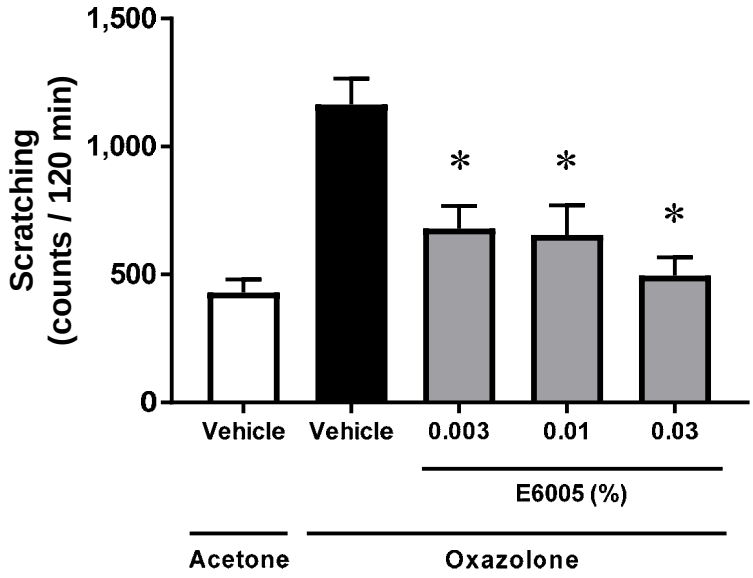

Fig. 2-3 Effect of E6005 on oxazolone-induced scratching behavior in NC/Nga mice. E6005 ointment (from 0.003 to 0.03%) or Vaseline-based vehicle ointment was applied on the ear of NC/Nga mice that were sensitized and challenged with oxazolone. Scratching behavior was induced 4–5 h after the administration of each compound and then evaluated for 120 min. Results are expressed as the mean ± S.E.M. (n = 24). * $P <$ 0.05 versus the vehicle-treated and oxazolone-challenged group.

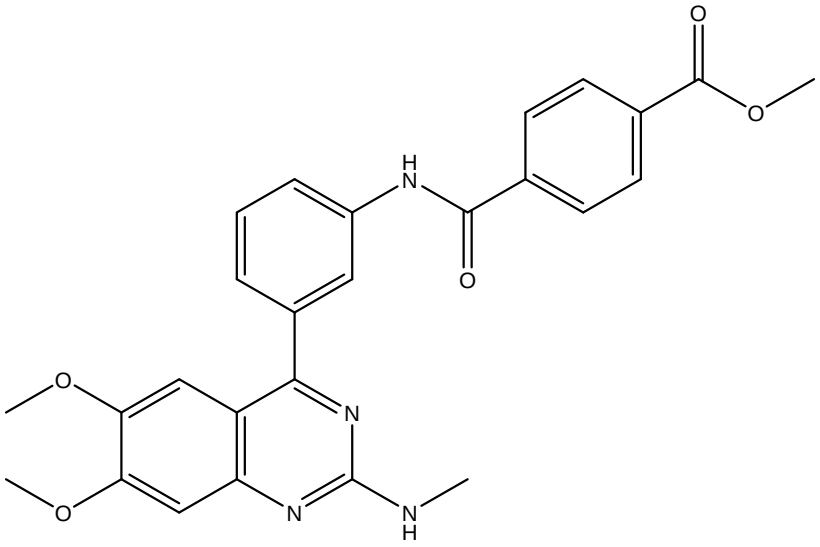

Fig. 2-4 Chemical structure of E6005.

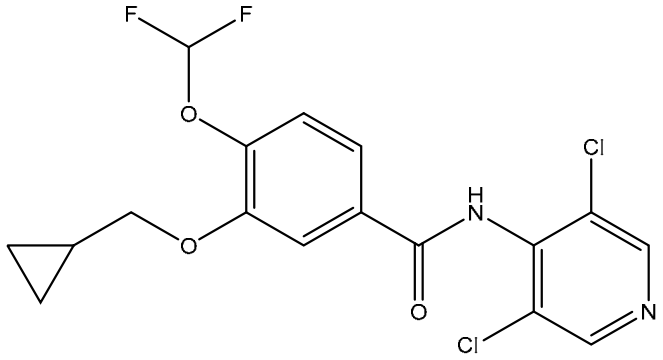

Fig. 2-5 Chemical structure of roflumilast.

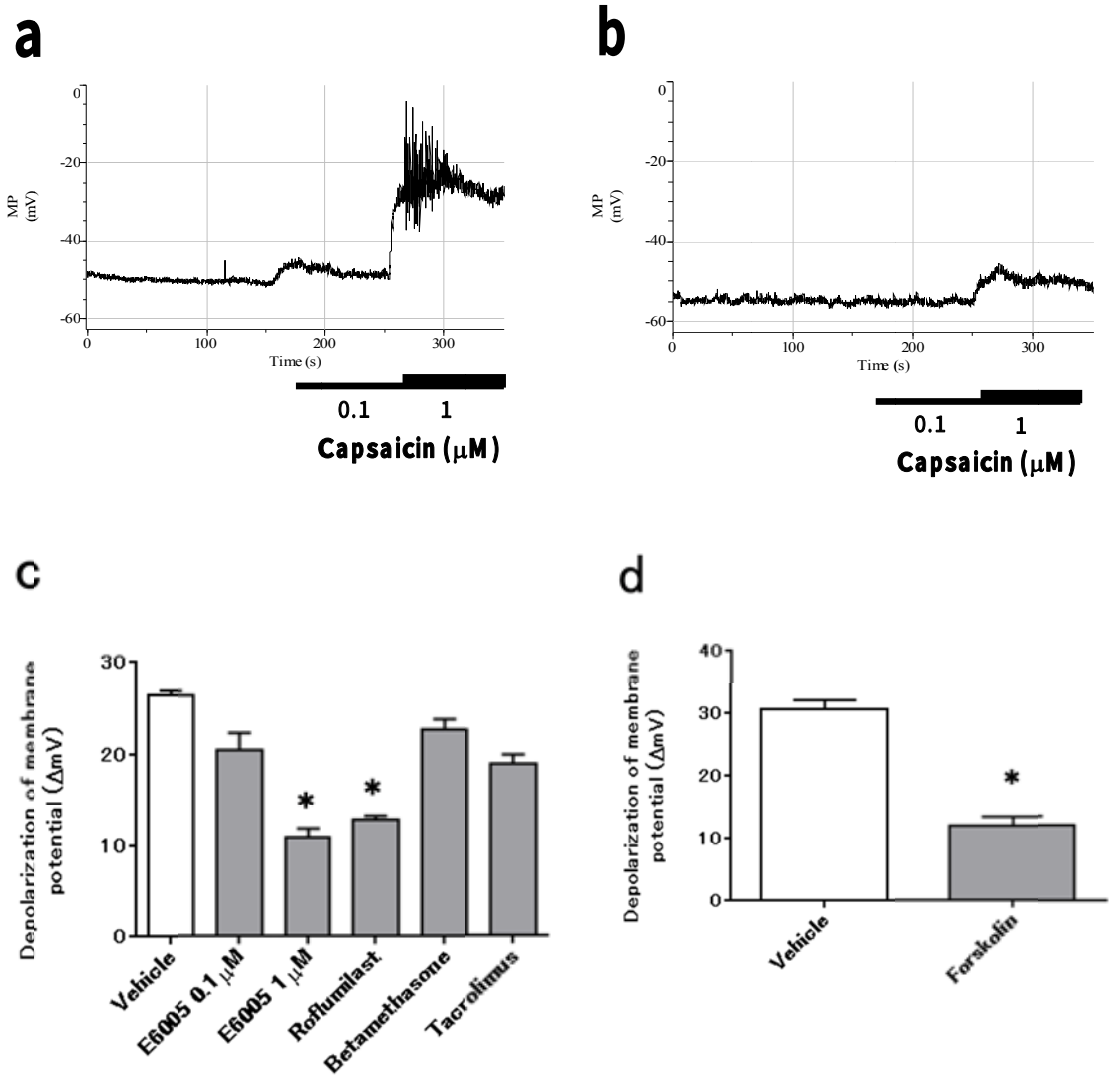

Fig. 2-6 Capsaicin-evoked depolarization in dorsal root ganglion (DRG) neurons and the inhibitory effect of compounds.

Tracings of membrane potential depicting capsaicin-elicited changes in membrane potential in rat DRG neurons recorded in the absence (a) or presence of E6005 (1 μM) (b) are shown. Capsaicin was applied as indicated by the horizontal bars. E6005 was applied 2 min before capsaicin stimulation. Comparison of the effects of E6005, roflumilast, betamethasone, tacrolimus, and forskolin in DRG neurons superfused with capsaicin is presented in (c) and (d). Changes in membrane potential (ΔmV) in (c) and (d) are the mean ± S.E.M. of n = 4–7 experiments. *$p < 0.05$ vs vehicle-treated DRG neurons.

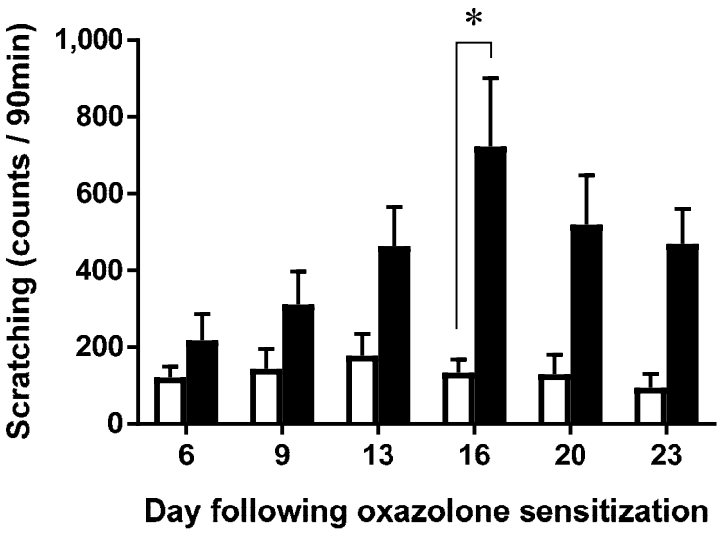

Fig. 2-7 Scratching behaviour in sensitized HR-1 mice induced by repeated application of oxazolone.

Starting 6 days following oxazolone-sensitization, HR-1 mice were administered acetone (vehicle; open bars) or oxazolone solution (solid bars) twice week by topical application to ear skin. The incidences of scratching were counted for 90 min, as described in the Materials and Methods. Results are expressed as mean ± S.E.M. of 8 mice. *$p < 0.05$ vs the acetone-challenged control group.

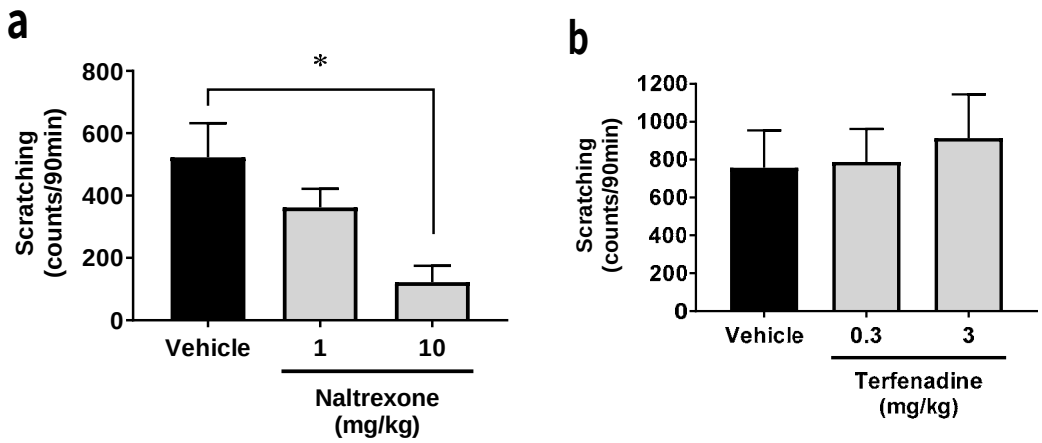

Fig. 2-8 Effects of μ-opioid receptor antagonist naltrexone and histamine H_1 receptor antagonist terfenadine on oxazolone-induced scratching behaviour in HR-1 mice.

Sensitized mice were repeatedly challenged with oxazolone, as described in Materials and Methods. (a) Naltrexone was injected subcutaneously before the 4th oxazolone challenge. (b) Terfenadine was orally administered before the 4th oxazolone challenge. Scratching behavior was induced 15 or 60 min after naltrexone or terfenadine administration, respectively. Incidences of scratching were counted for 90 min and the results expressed as mean ± S.E.M. of 8 mice. *$p < 0.05$ vs the vehicle-treated group.

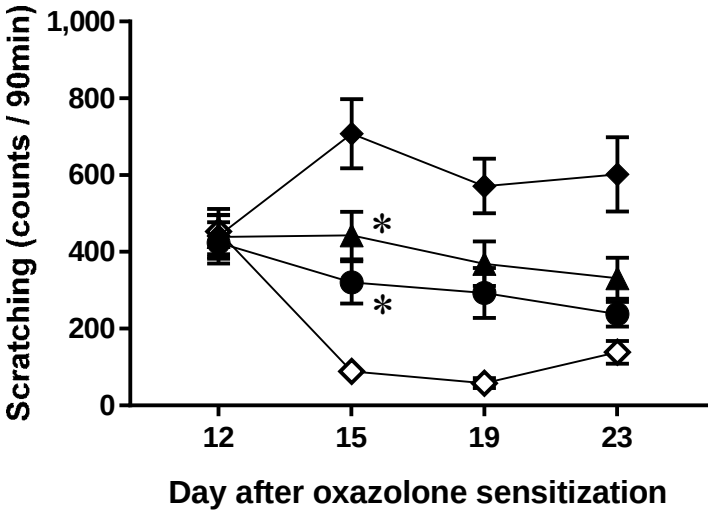

Fig. 2-9 Effect of E6005 on oxazolone-induced scratching behavior in HR-1 mice.
Sensitized HR-1 mice were repeatedly challenged on the ear with oxazolone twice a week as described in Fig. 2-5. (a) Vehicle ointment (solid diamonds), 0.01% (solid triangles), or 0.03% (solid circles) E6005 ointment was topically administrated before each oxazolone challenge performed 15, 19, and 23 days following sensitization. Vehicle ointment (open diamonds) was topically administrated before each acetone challenge performed 15, 19, and 23 days following sensitization. Scratching behavior was induced 4-5 h after the administration of each ointment and incidences of scratching were counted for 90 min. Results are expressed as mean ± S.E.M. of 32 mice. *$p < 0.05$ vs the vehicle-treated group on day 15.

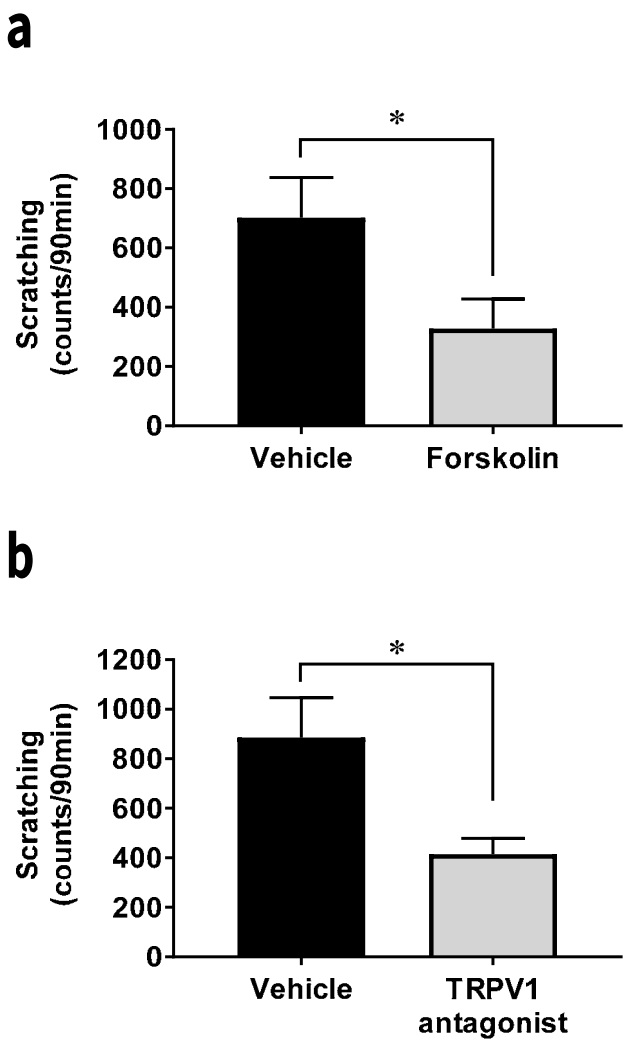

Fig. 2-10 Effect of E6005 on oxazolone-induced scratching behavior in HR-1 mice. Sensitized HR-1 mice were repeatedly challenged on the ear with oxazolone twice a week as described in Fig. 2-5. (a) Forskolin solution or vehicle (50% acetone/50% ethanol) was topically administrated before the 4th oxazolone challenge. Scratching behavior was induced 1 hour after the topical application, and counted for 90 min. Results are expressed as mean ± S.E.M. of 12 mice. *$p < 0.05$ vs the vehicle-treated group. (b) Sensitized mice were repeatedly challenged by application of oxazolone to the ear skin twice a week. TRPV1 antagonist JNJ17203212 (30 mg/kg) was orally administrated before the 4th oxazolone challenge. Scratching behavior was induced 1 hour after the administration and incidences of scratching counted for 90 min. Results are expressed as mean ± S.E.M. of 8 mice. *$p < 0.05$ vs the vehicle-treated group.

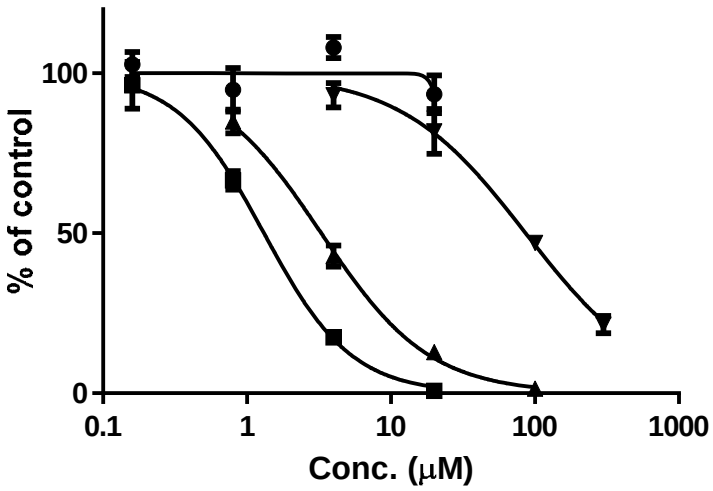

Fig. 2-11 Effects of E6005, amitriptyline, bupivacaine and lidocaine on Na current recorded for the hNav1.2-CHO cells.

Concentration-response curves obtained by train of 30 pulses in the presence of E6005 (solid circles), amitriptyline (solid squares), bupivacaine (solid triangles), or lidocaine (solid inverted triangles) were described. Mean ± S.E.M.

Chapter 3. Pharmacological assessment of CX3CR1 modulator E6130 as a therapeutic agent of IBD

3.1. Introduction

Inflammatory bowel disease is a group of idiopathic, chronic intestinal inflammatory diseases that primarily includes two distinct conditions: Crohn's disease and ulcerative colitis, which are both the result of inappropriate immune responses to antigens produced by commensal microorganisms. Although the signs of Crohn's disease and ulcerative colitis manifest primarily in the gastrointestinal tract, these diseases affect the entire human body [47]. Therapeutic treatments that inhibit cytokines are currently in widespread clinical use; however, the serious adverse events and lack of long-term efficacy of these treatments remain serious concerns.

Infiltration of leukocytes from the peripheral circulation into tissues such as the gut mucosa is an important aspect of immune surveillance. To enter the mucosal tissue from the blood, leukocytes must cross the endothelial barrier. They do this by interacting with cytokine- or other pro-inflammatory stimuli-activated endothelial cells *via* either leukocyte cell-surface chemokine receptors (and their respective endothelial and mucosal ligands) or *via* integrins and immunoglobulin superfamily cellular adhesion molecules [48, 49].

Chemokines and their receptors are also important means of orchestrating tissue-specific and cell type–selective leukocyte trafficking [50]. For example, fractalkine (also known as CX3C motif ligand 1: CX3CL1) is a chemokine prominently expressed by epithelial and endothelial cells that functions as both an adhesion molecule

and a chemotactic factor (Fig. 3-1) [51, 52]. Fractalkine binds to its sole receptor, CX3C chemokine receptor 1 (CX3CR1), which is expressed on the surfaces of monocytes, macrophages, dendritic cells, microglia, natural killer (NK) cells, and cytotoxic effector T-cells that contribute to the development of chronic inflammation [53, 54]. Apart from a role in post-ischemic brain injury, mice deficient in either fractalkine or CX3CR1, bred in a sterile environment, were phenotypically indistinguishable from wild type mice. In patients with inflammatory bowel disease, the expression of fractalkine by intestinal epithelial cells and microvascular cells and of CX3CR1 by peripheral blood T-cells increases with the level of disease activity. Thus, the fractalkine/CX3CR1 axis appears to be directly involved in the pathogenesis of inflammatory bowel disease [55 – 57].

In this chapter, I summarize *in vitro* and *in vivo* pharmacological profile of a novel CX3CR1 modulator E6130, which was identified from Eisai's small molecule compound libraries. I found that E6130 inhibited fractalkine-induced chemotaxis and induced down regulation of CX3CR1 on the cell surface in NK cells from human peripheral blood. E6130 also prevented the trafficking of CX3CR1-expressing leukocytes into colonic tissue in a murine $CD4^{+}CD45RB^{high}$ T cell–transfer colitis model, and it ameliorated other inflammatory bowel disease–related parameters in both the murine $CD4^{+}CD45RB^{high}$ T-cell-transfer colitis model and a murine oxazolone-induced colitis model. Together, these results suggest that E6130 is a promising agent for treating IBD.

3.2. Materials and Methods

3.2.1. Test compound and reagents

E6130 was synthesized by Eisai Co., Ltd. at its plant located in Kashima, Japan [6]. The chemical structure of E6130 is shown in Fig. 3-2. Oxazolone was purchased from Sigma-Aldrich (St. Louis, MO, USA). Recombinant human fractalkine was purchased from R&D Systems (Minneapolis, MN, USA).

3.2.2. Animals

BALB/c mice (female, 7–10 weeks old) were obtained from Charles River Laboratories Japan, Inc. (Tokyo, Japan). SCID mice (female, 6 weeks old) were obtained from CLEA Japan, Inc. (Tokyo, Japan). The mice were group-housed under controlled conditions (temperature, 22 ± 3 °C; humidity, 55% ± 5%; 12-h light/dark cycle) with *ad libitum* access to water and standard pelleted food.

All animal experiments were approved by the Committee for the Welfare of Laboratory Animals, Eisai Co. Ltd.

3.2.3. CX3CR1 down-regulation assay

Assay medium (RPMI 1640 medium containing 10% fetal bovine serum) (80 μL/well) and E6130 (10 μL/well) were added to each well of a 96-well culture plate. Written informed consent was obtained from each subject before blood draw. Human peripheral blood was drawn from the forearm vein of three healthy male volunteers and an aliquot (10 μL) was added to each well. After incubation for 30 min at 37 °C under an atmosphere of 5% CO_2, the human peripheral blood cells were washed twice with Flow cytometry (FCM) buffer (phosphate-buffered saline [PBS] containing 1% fetal

bovine serum, 1 mM EDTA, 0.1% bovine serum albumin). The cells were incubated with FcR Blocking Reagent (Miltenyi Biotec, Germany) for 10 min on ice to block Fc receptor and then stained for CD56 (NK cell surface marker) and CX3CR1 by incubation with allophycocyanin-conjugated anti-CD56 monoclonal antibody (Miltenyi Biotec, Germany) and phycoerythrin-conjugated anti-CX3CR1 monoclonal antibody (BioLegend, CA, USA), respectively, for 30 min on ice. The cells were then washed once and resuspended in FCM buffer. After incubation for 10 min on ice with 7-amino actinomycin D (Sigma-Aldrich, MO, USA) to discriminate dead cells, the fluorescence intensity of the stained cells was determined by using a FACSCanto cell analyzer (Becton Dickinson, NJ, USA). Loss of CX3CR1 staining on the cell surface was assumed to represent the induction of down-regulation of CX3CR1 on the cell surface. The mean fluorescence intensity (MFI) of the $CX3CR1^+$ cell population among the total NK cell population was also determined by using a FACSCanto cell analyzer. The percentage MFI of the control was determined by using the following formula:

$$\% \text{ MFI of control} = (MFI_{\text{test well}} - MFI_{\text{background well}}) / (MFI_{\text{control well}} - MFI_{\text{background well}}) \times 100,$$

where “test well” refers to wells containing E6130 and staining antibodies, “control well” refers to wells containing staining antibodies only, and “background well” refers to wells containing neither the staining antibodies nor E6130.

3.2.4. Isolation of NK cells from human peripheral blood

An aliquot (25 mL) of human peripheral blood was added to a plastic centrifugation tube containing 100 units of heparin sodium (Ajinomoto, Japan). An aliquot (8 mL) of physiological saline containing 6% dextran (Nacalai Tesque, Japan)

was added to the tube and the mixture was allowed to stand at room temperature for 30 min to allow sedimentation of the erythrocytes. The supernatant was transferred to another plastic centrifugation tube, mixed with an equivalent volume of PBS, and then centrifuged at 1,800 rpm for 7 min at room temperature. The resultant hemocyte fraction was suspended in 4 mL PBS and the suspension was superposed on 4 mL Ficoll-Paque Plus (GE Healthcare Life Sciences, Japan). After centrifugation of the suspension at 2,200 rpm for 30 min at room temperature, the cells in the intermediate layer (peripheral blood mononuclear cells) were collected, suspended in PBS, and centrifuged at 1,800 rpm for 7 min. The supernatant was removed and the precipitate was suspended in PBS containing 5 mM EDTA and 0.5% bovine serum albumin. NK cells were purified from the peripheral blood mononuclear cell population by means of negative selection using an NK cell isolation kit (Miltenyi Biotec, Germany) and a MACS LS column (Miltenyi Biotec, Germany). Cells passing through the column were considered NK cells and were collected, washed, and suspended in chemotaxis buffer (RPMI 1640 medium containing 10% fetal bovine serum, 50 μM 2-mercaptoethanol, and 10 mM HEPES).

3.2.5. Chemotaxis assay

Human fractalkine solution (solved in chemotaxis buffer, 60 μL/well) and chemotaxis buffer (480 μL/well) were added to the lower wells of a 24-well chemotaxis assay chamber (Boyden chamber, pore size: 5.0 μm) with final concentration of 0.2 nM. E6130 solution (60 μL/well) was also added to the lower wells. A mixture of NK cell suspension and E6130 was added to the upper wells and the chambers were incubated for 2 h at 37°C under an atmosphere of 5% CO_2. After incubation, the content of the

upper wells was discarded and the assay chambers were centrifuged at 1,800 rpm for 5 min. The supernatant was removed and a CellTiter-Glo reagent (Promega Corporation, Japan) was added to the precipitate. Chemiluminescence intensity was measured by using a Wallac 1420 ARVOsx multi-label counter (PerkinElmer Japan). The number of cells in each well was calculated by using a standard curve fitting the regression line for cell number. The percentage of cells exhibiting chemotaxis was determined by using the following formula:

$$\% \text{ of control} = (\text{cell number}_{\text{test well}} - \text{cell number}_{\text{blank well}}) / (\text{cell number}_{\text{control well}} - \text{cell number}_{\text{blank well}}) \times 100,$$

where "test well" refers to wells containing fractalkine and E6130, "blank well" refers to wells containing neither fractalkine nor E6130, and "control well" refers to wells containing fractalkine only.

3.2.6. GTPγS binding assay

Scintillation Proximity Assay (SPA) [^{35}S]GTPγS experiments were conducted using CHO-K1 membranes stably expressing human chemokine receptors incubated in assay buffer (20 mM HEPES [pH 7.4], 100 mM NaCl, 10 μg/mL saponin, 1 mM $MgCl_2$). In the agonistic activity assay, E6130 or reference ligand, assay buffer, CHO-K1 membrane - GDP mix, [^{35}S]GTPγS and WGA-PVT beads (Perkin Elmer, MA, USA) mix were successively added to the wells of an OptiPlate (Perkin Elmer, MA, USA). In the antagonistic activity assay, E6130 or reference ligand and CHO-K1 membrane-GDP mix were successively added to the wells of an OptiPlate and the plates were incubated for 15 min at room temperature. A reference agonist at its historical EC_{80} was then added, followed by the addition of [^{35}S]GTPγS and WGA-PVT beads.

In both assays, the plates were covered with a top seal, shaken on an orbital shaker for 2 min, and then incubated for 1 h at room temperature. The plates were then centrifuged for 10 min at 2,000 rpm and incubated at room temperature for 1 h. Each well was counted for 1 min by using a PerkinElmer TopCount reader (Perkin Elmer, MA, USA).

3.2.7. PathHunter β-arrestin recruitment assay

PathHunter is a trademark of DiscoveRx [58, 59]. PathHunter cell lines were expanded from freezer stocks in T25 flasks according to standard procedures and maintained in selective growth media before assay. Once it was established that the cells were healthy and growing normally, the cells were passaged from the flasks by using cell dissociation reagent and seeded into white-walled, clear-bottomed, 384-well microplates. Cells were seeded at a density of 5,000/well in a total volume of 20 μL and were allowed to adhere and recover overnight before the addition of E6130.

In the agonistic activity assay, intermediate dilutions of E6130 stock solutions were generated such that 5 μL of E6130 could be added to each well to produce a final concentration of DMSO of 1% of the total volume. The cells were incubated in the presence of E6130 at 37°C for 90 min.

In the antagonistic activity assay, agonist dose curves were constructed and used to determine EC_{80} values. Cells were pre-incubated with antagonist; this was followed by agonist challenge, as follows: 5 μL of E6130 was added to the cells and the plates were incubated at 37°C for 30 min. Then, 5 μL of agonist at its EC_{80} was added to the cells and the plates were incubated at 37°C for 90 min.

The assay signal was generated through the addition of 12.5 or 15 μL (50%, v/v)

of PathHunter Detection reagent cocktail for the agonistic and antagonistic activity assays, respectively, followed by incubation for 1 h at room temperature. The microplates were then read with a ParkinElmer EnVision multilabel plate reader (Perkin Elmer, MA, USA).

Dose curves in the presence of E6130 were plotted by using GraphPad Prism (GraphPad Software, CA, USA). In the agonistic activity assay, percentage activity was calculated by using relative light units (RLU) and the following formula:

% Activity = 100% × (mean $RLU_{test\ sample}$ − mean $RLU_{vehicle\ control}$) / (mean MAX $RLU_{control\ ligand}$ − mean $RLU_{vehicle\ control}$). In the antagonistic activity assay, percentage inhibition was calculated by using the following formula: % Inhibition = 100% × (1 – [mean $RLU_{test\ sample}$ − mean $RLU_{vehicle\ control}$] / mean $RLU_{EC80\ control}$ − mean $RLU_{vehicle\ control}$).

3.2.8. $CD4^+CD45RB^{high}$ T-cell preparation and T-cell-transfer colitis model

$CD4^+CD45RB^{high}$ T cells were isolated from BALB/c splenocytes. BALB/c mice were euthanized by means of cervical dislocation and their spleens were removed. The spleens were passed through a cell strainer (BD Biosciences, NJ, USA) and a single-cell suspension of splenocytes was prepared. After hemolysis, the $CD4^+$ T-cell population was purified from the splenocytes by means of negative selection by using a mouse $CD4^+$ T-cell Isolation Kit II (Miltenyi Biotec, Germany) and a MACS LS column. For the preparation of $CD4^+CD45RB^{high}$ T cells, the isolated total $CD4^+$ T cells were labeled with phycoerythrin-conjugated mouse anti-CD4 monoclonal antibody (eBioscience, CA, USA) and fluorescein isothiocyanate-conjugated mouse anti-CD45RB monoclonal antibody (eBioscience, CA, USA), and two-color cell sorting was performed by using a

FACSAria cell sorter (Becton Dickinson, NJ, USA). The sorted $CD4^{+}CD45RB^{high}$ T cells were suspended in PBS and intravenously transferred into SCID mice. After 2 weeks, E6130 or vehicle [0.5% methyl cellulose (0.5% MC)] was orally administered once daily to the SCID mice from day 14 to day 27. Stool consistency and body weight of all mice were recorded on days 14, 16, 18, 20, 22, 24, 26, and 28. On Day 28, the mice were euthanized, their colons were removed, and the weight and length of each colon was recorded. Stool consistency was scored as follows: (0) Normal, (1) Soft stool (well-formed pellets), (2) Soft stool (very soft but formed pellets), (3) Loose stool (pasty stool), and (4) Diarrhea (liquid stool that sticks to the anus). Relative body weight was calculated by using the following formula:

Relative body weight (%) = body weight (g) on day of measurement / body weight (g) on Day 14 × 100.

Next, the colons were washed with PBS and then incubated for 30 min at 37°C in PBS containing 1 mM dithiothreitol, 1 mM EDTA, and 1% fetal calf serum to remove epithelial cells. The remaining tissue was washed with PBS, cut into 1- to 2-mm sections, and incubated for 2.5 h at 37°C in RPMI 1640 containing 0.5 mg/mL collagenase A, 1 μg/mL DNase, and 5% fetal calf serum. After incubation, the suspension was passed through a cell strainer and the resultant cell suspension was centrifuged at 700 × *g* for 7 min at room temperature. The resultant enterocyte precipitate was suspended in 4 mL of PBS and the suspension was superposed on Percoll (GE Healthcare Life Sciences, IL, USA). After centrifugation at 700 × *g* for 20 min at room temperature, the cells in the intermediate layer were collected, suspended in PBS, and centrifuged at 700 × *g* for 7 min at 4°C. The supernatant was removed and the precipitate was suspended in FACS buffer (PBS containing 1 mM EDTA, 0.1%

bovine serum albumin, and 1% fetal calf serum). $CX3CR1^{+}$ cells were labeled with phycoerythrin-conjugated goat anti-CX3CR1 polyclonal antibody (R&D Systems, MN, USA) and the proportion of $CX3CR1^{+}$ cells was determined with a FACSCanto cell analyzer (Becton Dickinson, NJ, USA).

3.2.9. Pharmacokinetics and histological analysis in T-cell-transfer colitis model

For pharmacokinetic study, the sorted $CD4^{+}CD45RB^{high}$ T cells, as described above, were suspended in PBS and intravenously transferred into SCID mice. After 2 weeks, E6130 or vehicle was orally administered once daily to the SCID mice from Day 15 to Day 30. Blood samples were withdrawn at 30 min, 2 and 6 h after administration of E6130 on Day 29. After centrifugation of mouse blood, concentrations were quantitatively determined by a mass spectrometer equipped with a high performance liquid chromatography (HPLC) system.

For histological analysis, the colon was collected from mice on Day 30, fixed in 10% neutral buffered formalin, embedded in paraffin, and processed for microscopic examination of hematoxylin and eosin (H&E) stained sections.

3.2.10. Oxazolone-induced colitis model

BALB/c mice were sensitized with oxazolone on Day 0 by painting 3% oxazolone ethanol solution onto the skin of the abdomen. Five days after sensitization, oxazolone solution was intrarectally injected into the mice under isoflurane anesthesia to induce colitis. In vehicle group, ethanol/water (1:1) vehicle solution was intrarectally injected into the mice instead of oxazolone solution. E6130 was orally administered 1 h before intrarectal injection of oxazolone. The daily administration of E6130 continued

from Day 5 to Day 7. Two hours after the administration of E6130 on Day 7, the mice were euthanized by cervical dislocation, their colons were removed, and the length (mm) of the colons was recorded. Body weight ratio was calculated by using the following formula:

Body weight ratio (%) = (Body weight at Day 7) / (Body weight at Day 5) × 100.

3.2.11. Statistical analysis

Data are presented as means ± SEM. In stool score and relative body weight of a murine $CD4^+$ $CD45RB^{high}$ T-cell transfer colitis model, differences between $CD4^+CD45RB^{high}$ T-cell-transferred group and total-$CD4^+$ T-cells- or E6130-treated group were analyzed by repeated measures analysis of variance (RM-ANOVA) followed by Fisher's LSD test adjusted. In other parameters, differences between $CD4^+CD45RB^{high}$ T-cell-transferred group and total-$CD4^+$ T-cells- or E6130-treated group were analyzed by 1-way analysis of variance (ANOVA) followed by Fisher's LSD test. We used Bonferroni correction for a final multiple comparison to correct for inflation of type 1 error, and significance level was set to 0.001 (0.05 ÷ 48). In a murine oxazolone-induced-colitis model, differences between oxazolone-injected group and vehicle (ethanol/water)-injected or E6130-treated group were analyzed by 1-way analysis of variance (ANOVA) followed by Fisher's LSD test. We used Bonferroni correction for a final multiple comparison to correct for inflation of type 1 error, and significance level was set to 0.00625 (0.05 ÷ 8). Statistical analyses were performed by using GraphPad Prism (GraphPad Software, CA, USA).

3.3. Results

3.3.1. Effect of E6130 on fractalkine-induced chemotaxis by NK cells isolated from human peripheral blood

Previously, E6130 (Fig. 3-2) was identified from a G-protein coupled receptor (GPCR)-focused library by using a fluorometric microvolume assay technology scanner designed to perform high-throughput screening assays using multiwell plates. The library was screened by using an *in vitro* chemotaxis assay and an *in vivo* murine inflammatory bowel disease model.

A cell-based assay was used to assess the effects of E6130 on fractalkine-induced chemotaxis. Human NK cells were used, because most NK cells in human peripheral blood express CX3CR1 on their surfaces and NK cells can be easily isolated in large numbers. NK cells were incubated with E6130 for 2 h and chemotaxis was induced by incubation with fractalkine by using a multiwell chemotaxis chamber. Marked migration of NK cells was observed against 0.2 nM fractalkine (number of cells in blank well: 887 ± 324, number in fractalkine-containing well: 8,615 ± 2,936). However, E6130 inhibited the chemotaxis of NK cells, with an IC_{50} value of 4.9 nM (Fig. 3-3a).

3.3.2. Effect of E6130 on CX3CR1 down-regulation on the cell surface of human peripheral blood NK cells

E6130 exhibited no antagonistic activity on [^{35}S]GTPγS binding *via* CX3CR1 (Table 1). Therefore, I hypothesized that E6130 prevents fractalkine from binding to the receptor by inducing down-regulation of CX3CR1 on the cell surface, leading to inhibition of the fractalkine-induced chemotaxis of human leukocytes. To test this hypothesis, human peripheral blood was incubated with E6130 for 30 min at 37°C and

then stained with monoclonal antibodies to CD56 and CX3CR1. The fluorescence intensity of CX3CR1 on $CD56^+$ NK cells was evaluated by means of flow cytometry. E6130 induced the down-regulation of CX3CR1 on the cell surface of $CD56^+$ NK cells with an EC_{50} value of 5.2 nM (Fig. 3-3b).

3.3.3. Effect of E6130 on GTPγS binding *via* CX3CR1

When activated, CX3CR1 changes conformation to expose a G-protein complex binding site. Once this G-protein complex is bound, the G_α subunit releases GDP and binds GTP. Agonist-activated GPCR induces receptor phosphorylation mediated by GPCR kinases, leading to the recruitment of β-arrestin. Upon receptor phosphorylation and β-arrestin binding, most GPCRs internalize into clathrin-coated vesicles. Therefore, next I examined the effects of E6130 on [^{35}S]GTPγS binding and β-arrestin recruitment by CX3CR1 in CX3CR1-expressing CHO-K1 membrane. E6130 had agonistic activity with respect to [^{35}S]GTPγS binding (EC_{50} = 133 nM) and β-arrestin recruitment (EC_{50} = 2.4 μM) through CX3CR1 (Fig. 3-4ab). No antagonistic activity of E6130 was observed in the presence of fractalkine (IC_{50} value: >10 μM).

The agonistic and antagonistic activities of E6130 with respect to [^{35}S]GTPγS binding and β-arrestin recruitment were also examined by using CHO-K1 membrane expressing human chemokine receptors. E6130 had agonistic activity through chemokine orphan receptor 1 for β-arrestin recruitment at 10 μM. However, no significant agonistic or antagonistic activity (EC_{50} and IC_{50} values: >10 μM) of E6130 was observed with respect to [^{35}S]GTPγS binding or β-arrestin recruitment through any other chemokine receptor (Tables 3-1, 3-2).

3.3.4. Effects of E6130 in a murine $CD4^+CD45RB^{high}$ T-cell-transfer colitis model

The etiology of IBD is still not clear. In general, the major cause is dysregulation of immune responses induced by environmental or genetic factors. Thus, many genetically modified mouse models, chemical-induced models, and the T cell-transfer model have been established for IBD study. All these animal models indicate that the T cell-mediated autoimmune response plays an important role. In these IBD animal models, transfer of $CD4^+CD45RB^{high}$ T-cell into congenic immunodeficiency mice, which is known as a good Crohn's disease model, is one of the most common models.

The *in vivo* efficacy of E6130 after oral administration was assessed by using a murine $CD4^+CD45RB^{high}$ T-cell-transfer colitis model. E6130 (10 or 30 mg/kg) was orally administered to the SCID mice once a day. Oral availability of E6130 was confirmed with pharmacokinetic study in the mice (Table 3-3). The total $CD4^+$ T-cell population was used as the negative control. Stool consistency and body weight were recorded, and colons were excised and their weight and length were determined because colon length-to-weight ratio correlates well with histopathological scores [60]. The number of $CX3CR1^+$ leukocytes in the lamina propria was determined by means of flow cytometry. Oral administration of E6130 significantly ($p < 0.001$) improved stool consistency from Day 18 at doses of 10 and 30 mg/kg compared with $CD4^+CD45RB^{high}$ T-cell-transferred group, and significantly ($p < 0.001$) ameliorated body weight loss from Day 22 at doses of 10 and 30 mg/kg (Fig. 3-5ab). Furthermore, oral administration of E6130 significantly ($p < 0.001$) ameliorated the increased colon weight to length ratio as well as the increase in the number of $CX3CR1^+$ leukocytes in the lamina propria at doses of 10 and 30 mg/kg (Fig. 3-6ab). These effects of E6130 were histopathologically confirmed by a marked reduction in mucosal thickness due to much less inflammatory

cell infiltration and crypt hyperplasia in treated animals (Fig. 3-7ab).

3.3.5. Effects of E6130 in a murine oxazolone-induced-colitis model

Oxazolone-induced colitis is a T cell-driven colitis characterized by a strong innate granulocytic response. The *in vivo* efficacy of E6130 after oral administration was assessed in a murine oxazolone-induced-colitis model. Body weight loss and shrinkage of the colon are well recognized as features of hapten-induced colitis model [61, 62]. At a dose of 30 mg/kg, E6130 significantly ($p < 0.00625$) prevented the colon-length shortening, and significantly ($p < 0.00625$) suppressed the body weight loss on day 7 (Fig. 3-8ab).

3.4. Discussion

IBD such as Crohn's disease and ulcerative colitis are characterized by a chronic clinical course of relapse and remission. In both Crohn's disease and ulcerative colitis, leukocyte infiltration into the intestine is a fundamental event in the development and progression of the disease. Indeed, $CX3CR1^{+}CD4^{+}$ T cells are increased in the peripheral blood and inflamed tissues of patients with IBD. Fractalkine is expressed by epithelial cells in the colonic tissue and the expression is greater in the inflamed tissues of patients with Crohn's disease or ulcerative colitis [56], suggesting that the fractalkine/CX3CR1 axis plays an important role in the pathogenesis of IBD. Therefore, inhibition of the trafficking of $CX3CR1^{+}$ leukocytes represents a potential means of treating IBD.

I found here that E6130 had an inhibitory activity against fractalkine-induced chemotaxis in NK cells isolated from human peripheral blood. The down-regulation of CX3CR1 on the cell surface induced by E6130 mainly contribute to the inhibition of fractalkine-induced chemotaxis, because the down-regulation of CX3CR1-inducing activity of E6130 (EC_{50} = 5.2 nM) was more potent than its agonistic activity with respect to GTPγS binding (EC_{50} = 133 nM) and β-arrestin recruitment (EC_{50} = 2.4 μM). E6130 exhibited no antagonistic activity on [^{35}S]GTPγS binding *via* CX3CR1. I cannot completely ruled out the possibility that E6130 acts through a mechanism other than CX3CR1, because E6130 was shown to affect ACKR3/CMKOR1 in β-arrestin recruitment at the high concentration of E6130 (10 μM) (Table 3-2). *In vitro* data suggested that E6130 induced down-regulation of CX3CR1 on the cell surface, thereby inhibiting the interaction between fractalkine and CX3CR1, leading to inhibition of fractalkine-induced chemotaxis.

Numerous efforts have been made to clarify the *in vivo* role of the fractalkine/CX3CR1 axis in intestinal inflammation; however, it remains unclear whether the fractalkine/CX3CR1 axis contributes to the progression of colitis. Kostadinova *et al.* demonstrated that knockout of *CX3CR1* in mice suppressed the development of dextran sulfate sodium–induced colitis and inhibited the trafficking of inducible nitric oxide synthase–expressing macrophages into the mucosa [63]. Likewise, Niess and Adler demonstrated in a $CD4^+$ T-cell adoptive-transfer colitis model that $CX3CR1^{gfp/gfp}/RAG2^{-/-}$ mice had less colitis signs than $RAG2^{-/-}$ mice, fewer dendritic cells in the mesenteric lymph nodes, and reduced serum interferon gamma and interleukin 17 concentrations [64]. In contrast, Medina-Contreras *et al.* demonstrated that deletion of *CX3CR1* aggravates the signs of colitis in mice [65], and Kayama *et al.* demonstrated the importance of intestinal $CX3CR1^{high}$ myeloid cells for the prevention of intestinal inflammation [66]. These inconsistent results may be due to a lack of expression of CX3CR1 in a specific stage during fetal development or an excessive compensation by other chemokine pathway or, a possibility that both too much and too little receptor might predispose to pathology. Therefore, to fully understand the mechanistic role of the fractalkine/CX3CR1 axis in intestinal inflammation, the fractalkine/CX3CR1 axis needs to be interrupted at the exact time at which inflammation begins. Here, in a murine $CD4^+CD45RB^{high}$ T-cell-transfer colitis model, I used E6130 to interrupt the fractalkine/CX3CR1 axis during intestinal inflammation and found that E6130 suppressed the signs of colitis by inhibiting the infiltration of $CX3CR1^+$ leukocytes into inflamed colon tissue.

Massive infiltration of leukocytes—including lymphocytes, macrophages, and neutrophils—into inflamed colonic mucosa is a hallmark of human IBD [49, 50]. In this

regard, chemokine/receptor axes play central roles in the trafficking of leukocytes from the blood into inflamed intestinal mucosa [50]. Previous studies have also shown the importance of the chemokine/receptor axes in the onset of T-cell-dependent, hapten-induced experimental colitis [67, 68]. Khan *et al.* reported the critical role of monocyte chemoattractant protein-1 (MCP-1) in a dinitrobenzenesulfonic acid-induced colitis model [69]. MCP-1 is a ligand for CCR2, CCR4, and CCR11, and these receptors are expressed by monocytes, macrophages, and certain subsets of T lymphocytes. Khan *et al.* revealed that knockout of the gene encoding MCP-1 in mice attenuates the onset and severity of the signs of colitis by reducing the infiltration of $F4/80^+$ macrophages and $CD3^+$ lymphocytes into inflamed mucosa [67]. Most chemokines, including MCP-1, can bind to several receptors, and most receptors bind many chemokines; however, fractalkine binds only to CX3CR1. Because the expression of MCP-1 mRNA is significantly decreased in CX3CR1-deficient mice compared with in wild-type mice, it is possible that E6130 suppresses the expression of MCP-1 in inflamed colonic tissues [69]. This suggests that the fractalkine/CX3CR1 axis exists upstream of other chemokine/receptor axes that together form a specialized system that regulates chemokine-induced leukocyte infiltration into the colonic mucosa.

In conclusion, here I characterized E6130, a novel CX3CR1 modulator. I found that E6130 induced down-regulation of CX3CR1 on the cell surface, leading to suppression of fractalkine-induced chemotaxis of $CX3CR1^+$ human NK cells. Oral administration of E6130 ameliorated inflammatory bowel disease-related parameters in both a murine $CD4^+CD45RB^{high}$ T-cell-transfer colitis model and a murine oxazolone-induced colitis model. In the murine $CD4^+CD45RB^{high}$ T-cell-transfer colitis model, E6130 inhibited the trafficking of $CX3CR1^+$ immune cells into the mucosa and

decreased the number of these cells in the gut mucosal membrane. Thus, E6130 is a potentially useful therapeutic agent for treatment of IBD such as ulcerative colitis and Crohn's disease.

Table 3-1. Agonistic and antagonistic activities of E6130 (10 μmol/L) towards chemokine receptors in GTPγS binding

[^{35}S]GTPγS binding[a], Agonist mode		[^{35}S]GTPγS binding[a], Antagonist mode	
Receptor	% Activation[b]	Receptor	% Inhibition[c]
CCR1	1.6	CCR1	15.1
CCR2	3.1	CCR2	24.9
CCR3	−8.1	CCR3	54.8
CCR4	−6.1	CCR4	44.0
CCR6	−5.2	CCR6	18.7
CCR7	0.9	CCR7	−15.2
CCR8	8.9	CCR8	9.7
CCR10	−5.1	CCR10	9.1
CX3CR1	95.2	CX3CR1	-18.6
CXCR1	−2.2	CXCR1	23.3
CXCR2	−3.4	CXCR2	9.1
CXCR3	2.4	CXCR3	22.7
CXCR4	0.0	CXCR4	13.2
CXCR6	−1.3	CXCR6	10.9
XCR1	−4.3	XCR1	23.8

[a] GTPγS binding assay was performed for chemokine receptors.

[b] Agonist activity of E6130 is expressed as a percentage of the activity of the reference agonists at their EC_{100} concentrations. Negative values indicate antagonistic activities.

[c] Negative values indicate agonistic activities.

Table 3-2. Agonistic and antagonistic activities of E6130 (10 μmol/L) towards chemokine receptors in β-arrestin recruitment

β-arrestin[a], Agonist mode		β-arrestin[a], Antagonist mode	
Receptor	% Activation[b]	Receptor	% Inhibition[c]
CCR2	−3	CCR2	−13
CCR3	−2	CCR3	5
CCR4	−2	CCR4	−11
CCR5	−2	CCR5	0
CCR6	−2	CCR6	2
CCR7	−5	CCR7	10
CCR8	−1	CCR8	15
CCR9	−3	CCR9	6
CCR10	−1	CCR10	−15
CX3CR1	179	CX3CR1	0
CXCR1	−1	CXCR1	−10
CXCR2	−1	CXCR2	6
CXCR3	−1	CXCR3	−2
CXCR4	3	CXCR4	10
CXCR5	−2	CXCR5	4
CXCR6	1	CXCR6	−10
ACKR3/CMKOR1	157	ACKR3/CMKOR1	0

[a] PathHunter β-arrestin assay was performed for chemokine/chemokine-like receptors.

[b] Agonist activity of E6130 is expressed as a percentage of the activity of the reference agonists at their EC_{100} concentrations. Negative values indicate antagonistic activities.

[c] Negative values indicate agonistic activities.

Table 3-3. Plasma concentrations of E6130 after oral administration in mice

Dose (mg/kg)	Plasma concentration (nM)		
	0.5 h	2 h	6 h
10	236 ± 57.3	26.4 ± 11.6	10.7 ± 5.24
30	1,430 ± 237	65.8 ± 12.6	22.8 ± 15.9

Data are shown as the mean values ± S.E.M. (n = 3-6).

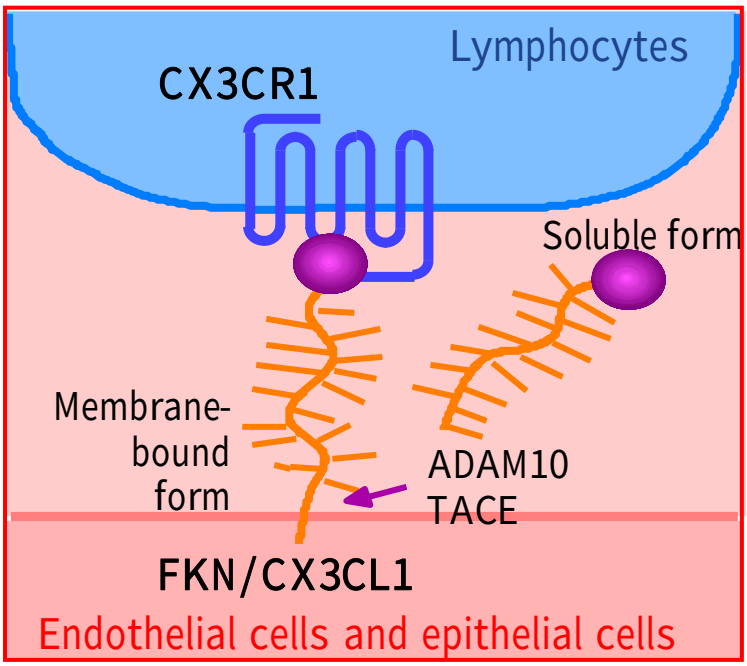

Fig. 3-1 Fractalkine/CX3CL1 and CX3CR1.

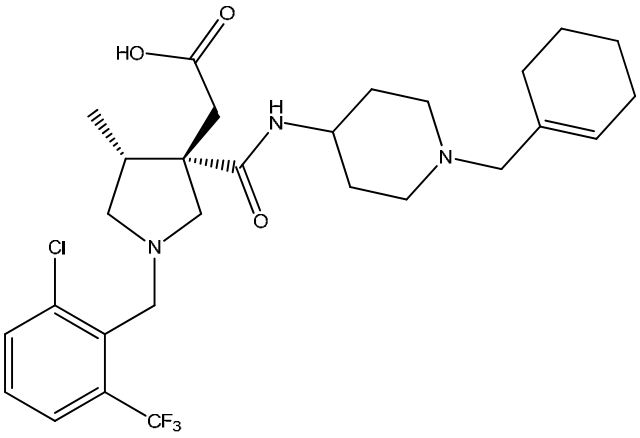

Fig. 3-2 Chemical structure of E6130.

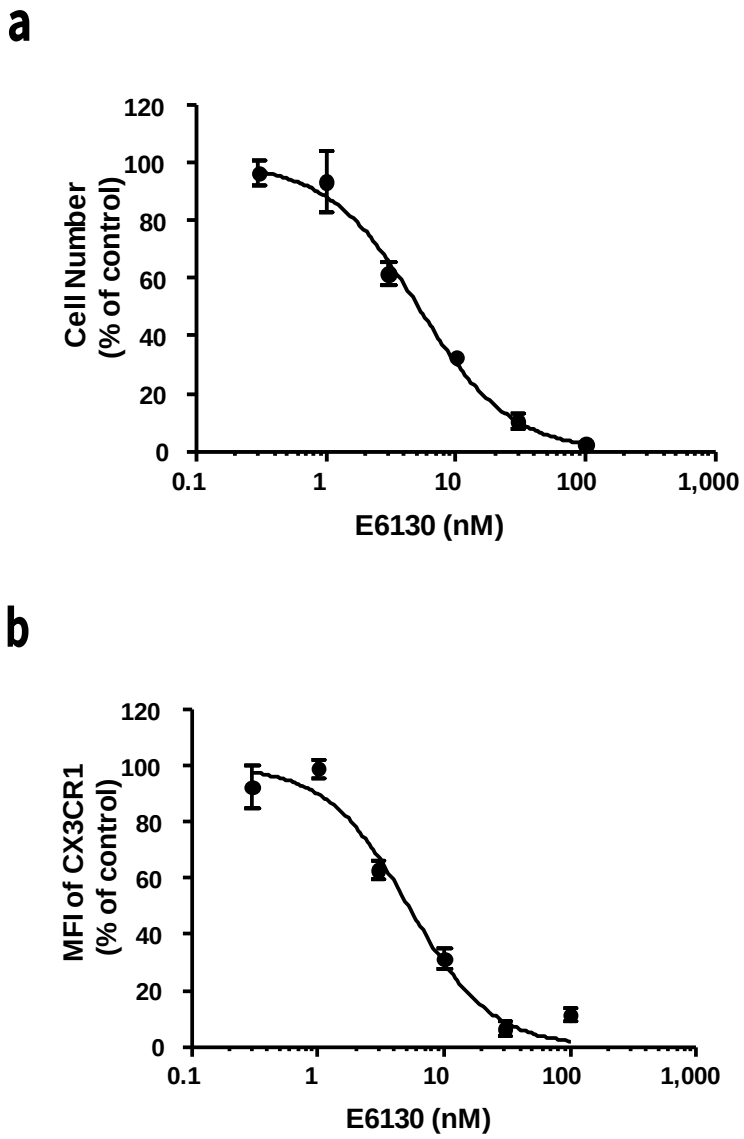

Fig. 3-3 Effects of E6130 on fractalkine-induced chemotaxis and down-regulation of CX3CR1 on the cell surface in human peripheral blood natural killer cells.

(a) Effects of E6130 on fractalkine-induced chemotaxis in human peripheral blood natural killer cells. Data are presented as means ± S.E.M. from three independent experiments performed in duplicate for the blank and control groups, and performed in a single well for the test compound group. (b) Effects of E6130 on the induction of down-regulation of CX3CR1 on the cell surface in human peripheral blood natural killer cells.

Data are presented as means ± S.E.M. (n = 3). MFI, mean fluorescence intensity.

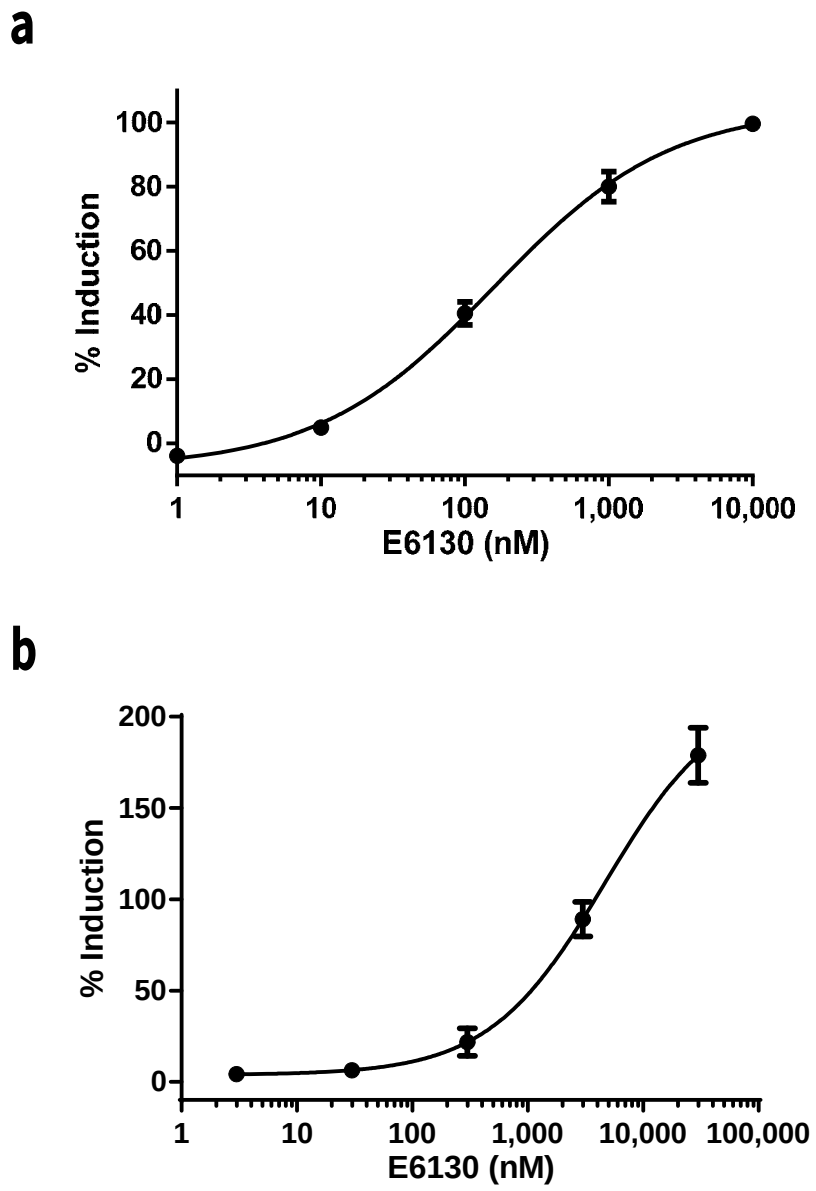

Fig. 3-4 Agonistic activity of E6130 against CX3CR1 with respect to GTPγS binding and β-arrestin recruitment.

Agonistic activity of E6130 against CX3CR1 in (a) [^{35}S]GTPγS binding assay and (b) β-arrestin recruitment assay. The agonistic activity of E6130 is expressed as a percentage of the activity of the reference agonist (fractalkine) at its EC_{100} concentration.

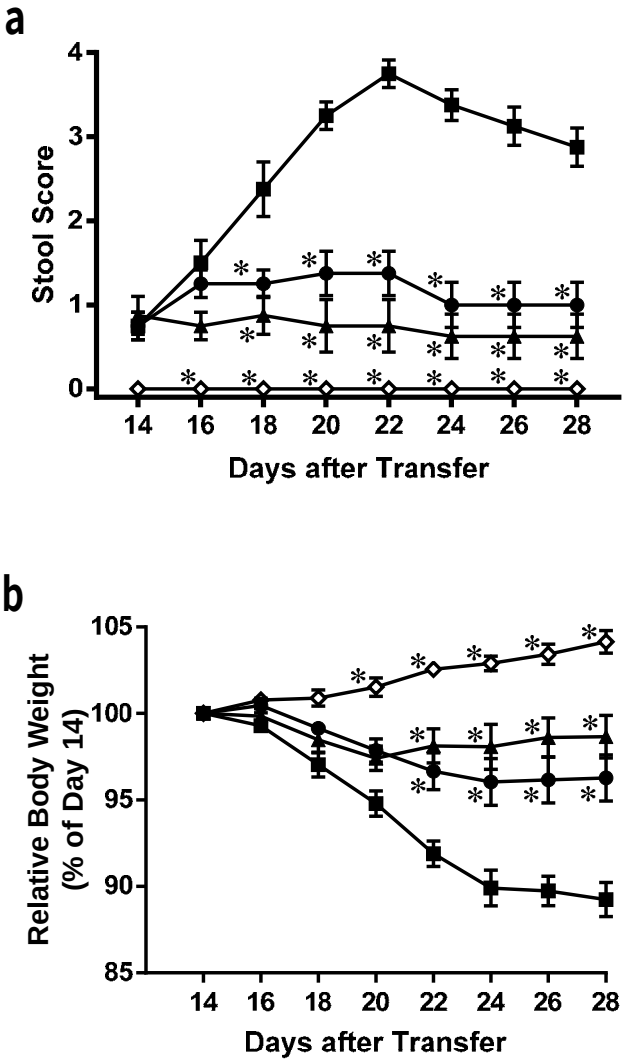

Fig. 3-5 Effect of E6130 in a murine $CD4^{+}CD45RB^{high}$ T-cell-transfer colitis model.
(a) Stool score was assessed on the indicated days in $CD4^{+}CD45RB^{high}$ T-cell-transfer mice given vehicle (solid squares), 10 mg/kg E6130 (solid circles), 30 mg/kg E6130 (solid triangles), or total $CD4^{+}$ T cells (open diamonds). (b) $CD4^{+}CD45RB^{high}$ T-cell-transfer mice were administered vehicle (solid squares), 10 mg/kg E6130 (solid circles), or 30 mg/kg E6130 (solid triangles). Mice that received total $CD4^{+}$ T cells were treated with vehicle (open diamonds). Body weight is expressed as the percentage of that at Day 14. Results are presented as means ± S.E.M. (n = 8/group). $*p < 0.001$ versus vehicle in $CD4^{+}CD45RB^{high}$ T-cell-transferred group (repeated measures analysis of variance (RM-ANOVA) followed by Fisher's LSD test in each time slice).

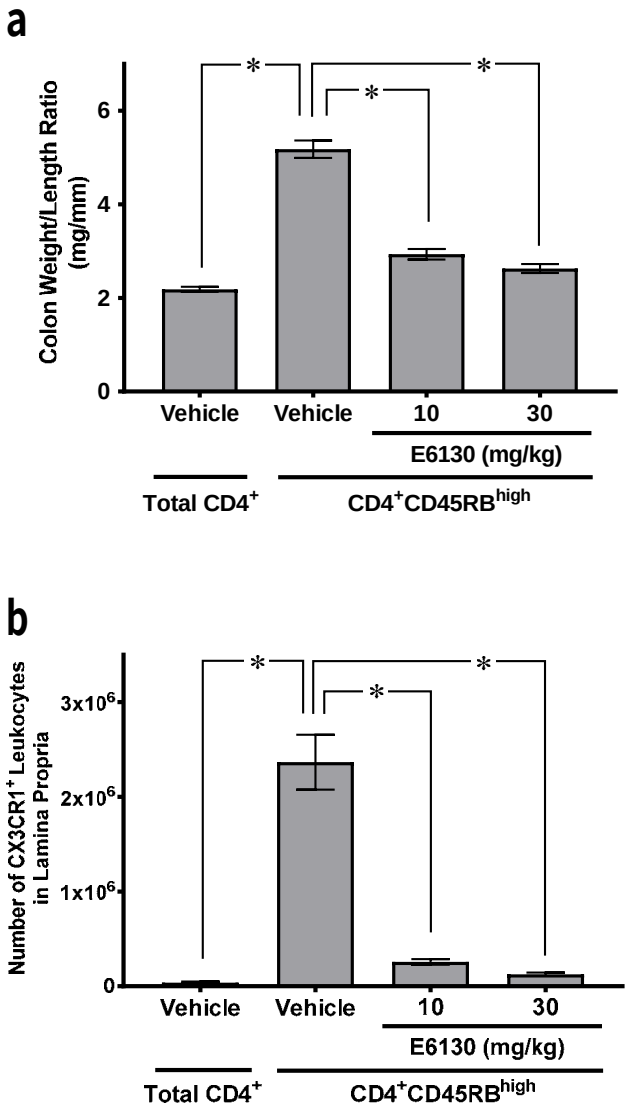

Fig. 3-6 Effect of E6130 in a murine $CD4^{+}CD45RB^{high}$ T-cell-transfer colitis model.
(a) The colon weight to length ratio of each mouse was assessed on Day 28 after T-cell transfer. (b) On Day 28 after T-cell transfer, the mice were euthanized and the colons were excised. Leukocytes were extracted from the colon tissue by using collagenase. $CX3CR1^{+}$ cells were labeled with phycoerythrin-conjugated anti-CX3CR1 antibody and the size of the $CX3CR1^{+}$ cell population was determined by using a FACSCanto cell analyzer. Results are presented as means ± S.E.M. (n = 8/group). *$p < 0.001$ versus vehicle in $CD4^{+}CD45RB^{high}$ T-cell-transferred group (1-way ANOVA followed by Fisher's LSD test).

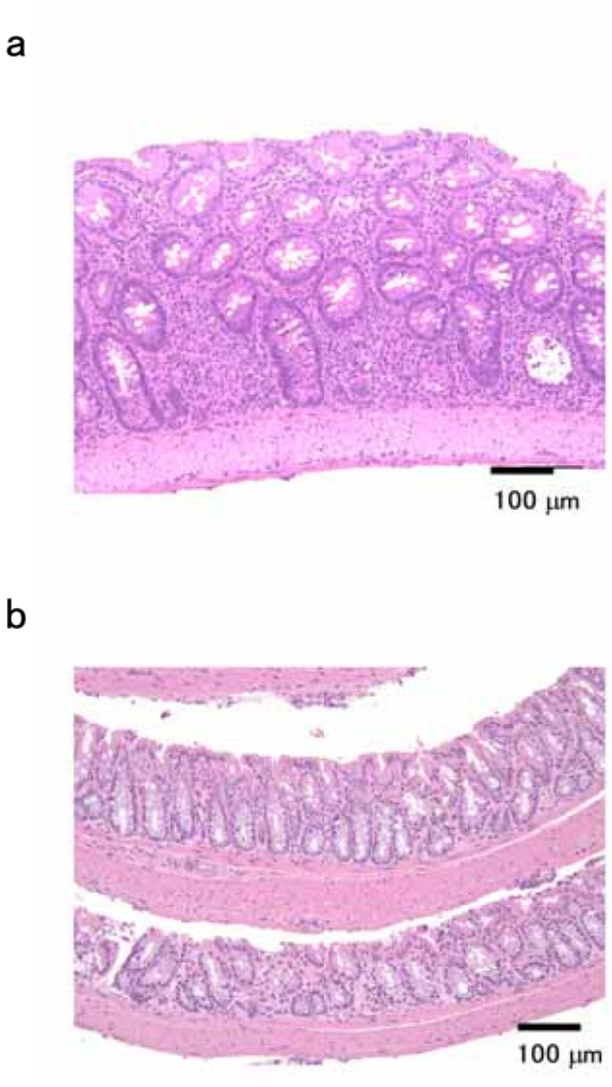

Fig. 3-7 Effect of E6130 in a murine $CD4^{+}CD45RB^{high}$ T-cell-transfer colitis model. Histopathology of colon from vehicle (a) or E6130 at 30 mg/kg (b) treated $CD4^{+}CD45RB^{high}$ T-cell-transfer colitis model. Massive thickening of intestinal mucosa with inflammatory cell infiltration and reactive hyperplasia of mucosal epithelial cells with cell debris in the glandular lumen of the vehicle treated animal and almost normal structure of colon in the E6130 treated animal. Bars 100 μm. H&E stain.

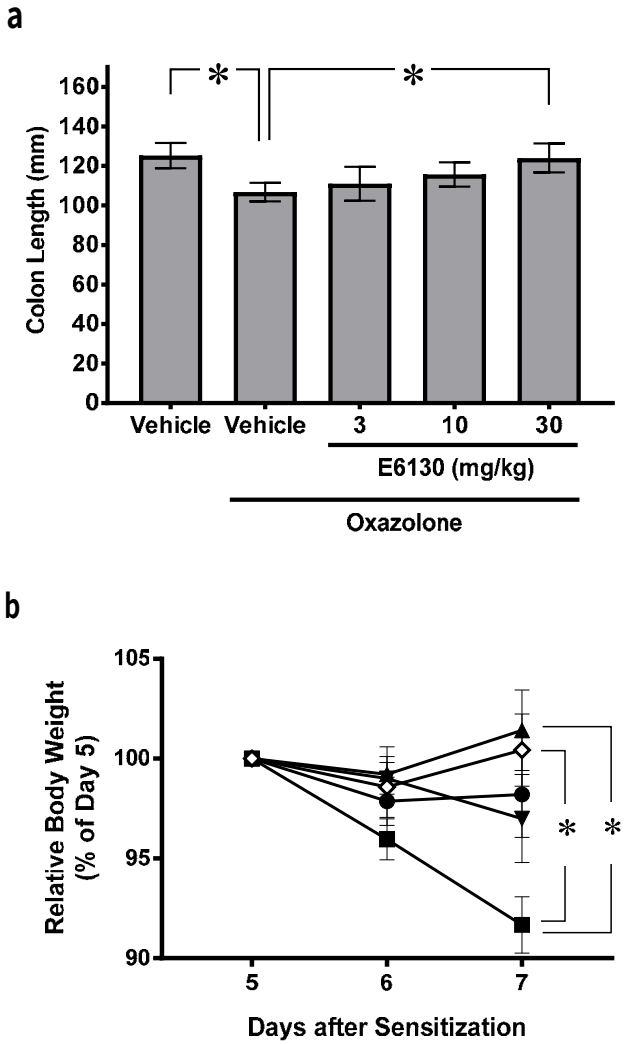

Fig. 3-8 Effect of E6130 in a murine oxazolone-induced colitis model.

(a) Mice were euthanized, colons were excised, and colon length was measured. (b) Mice that intrarectally received oxazolone solution were administered vehicle (0.5% MC solution) (solid squares), 3 mg/kg E6130 (solid inverted triangles), 10 mg/kg E6130 (solid circles), or 30 mg/kg E6130 (solid triangles). Mice that received same vehicle (ethanol/water) were treated with vehicle (0.5% MC solution) (open diamonds). Body weight is expressed as the percentage of that at Day 5. Data are presented as means ± S.E.M. (n = 9/group). *$p < 0.00625$ versus vehicle in oxazolone-injected group (1-way analysis of variance (ANOVA) followed by Fisher's LSD test).

Chapter 4. Concluding Remarks

To discover better drug candidate agents for the treatment of atopic dermatitis and IBD, screening of Eisai's small molecule compound libraries was conducted. E6005 and E6130 were identified through compound screening and chemical optimization of hit/lead compounds. The aims of this investigation is to elucidate whether it is worth that the candidate compounds, which were identified from the screening and chemical optimization, introduce clinical.

As described in chapter 2, I first examined an inhibitory effect of E6005, a newly synthesized PDE4 inhibitor, on depolarization of C-fiber neuron which mediates the itch sensation. Results showed that E6005 suppressed C-fiber depolarization and indicates that this effect may lead to *in vivo* anti-pruritic effect. On the basis of this characteristic, an inhibitory effect of E6005 was investigated on oxazolone-induced scratching behavior in mice. Topical application of E6005 immediately inhibits itching behavior, suggesting that inhibitory effects of E6005 on depolarization of C-fiber neuron may (at least in part) contribute to the immediate anti-pruritic effect of E6005. E6005 reduces oxazolone-induced skin inflammation in mice. This anti-inflammatory effect of E6005 is due to not only inhibitory effect of cytokine production such as IL-2, IL-4, IL-12, IFN-γ and TNF-α but also inhibitory effect on the excitation of C-fiber neuron. Recently, topical application of E6005 has been shown to ameliorate skin inflammation and itching in Japanese adult patients with atopic dermatitis. To date, a variety of systemic PDE4 inhibitors have been developed. However, side effects such as particularly nausea and vomiting hamper their clinical utility. Emetic effect of E6005 are actually lower than that of cilomilast, a well-known PDE4 inhibitor, because E6005 have been

originally designed to lower the emetic action. Furthermore, the quite low blood concentration of E6005 through a topical application will enable a good systemic tolerability. Actually, topical application of E6005 ointment for up to 12 weeks was well tolerated in Japanese patients with atopic dermatitis [70, 71].

In chapter 3, I assessed *in vitro* and *in vivo* pharmacological characteristics of E6130, a novel CX3CR1 modulator derived from Eisai's GPCR focused libraries. In natural killer (NK) cells obtained from human peripheral blood, E6130 inhibited CX3CL1-induced chemotaxis with IC_{50} value of 4.9 nM. E6130 induced down regulation of CX3CR1 in human NK cells with EC_{50} value of 5.2 nM. *In vitro* data suggests that E6130 induces down regulation of CX3CR1 and thus inhibits interaction between CX3CL1 and CX3CR1. Such mechanism would lead to the inhibition of CX3CL1-induced chemotaxis. In a murine $CD4^+$ $CD45RB^{high}$ T-cell transfer-induced colitis model, oral administration of E6130 decreased body weight loss and improved the score of stool consistency. In addition, E6130 significantly ameliorated colon weight/length ratio and the number of $CX3CR1^+$ leukocytes in the lamina propria. In an oxazolone-induced colitis model, E6130 significantly inhibited both colon length shortening and body weight loss. These results suggest that E6130 is a promising novel therapeutic agent for the treatment of IBD.

As summary of this dissertation, I summarize important findings in current investigation as follows; i) E6005, PDE4 selective inhibitor, and E6130, CX3CR1 modulator, were discovered from small molecule compound libraries created by Eisai, ii) E6005 and E6130 are promising therapeutic agents for treatment of atopic dermatitis and IBD, respectively, iii) clinical introduction of these compounds were achieved. Taken together, these finding show that developmental possibility of these compounds

for treatment of inflammatory diseases, and they have significant potential to offer innovative solution as effective therapeutics. I strongly hope that my investigation will lead to make drugs that fulfill the needs of patients and improve welfare of people in the world.

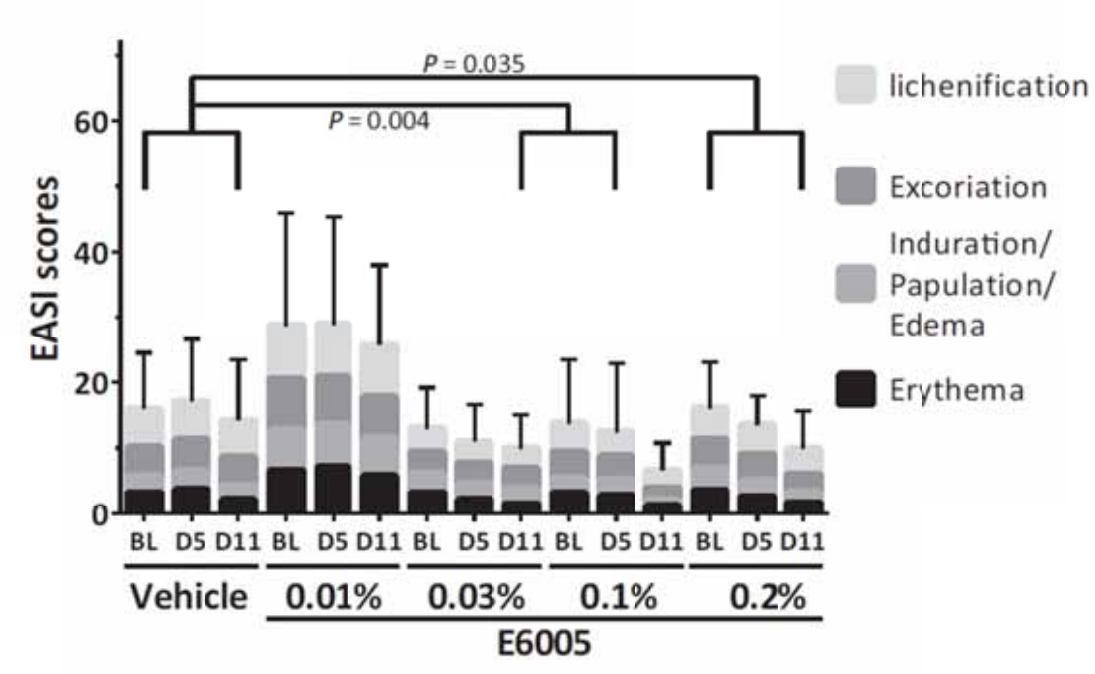

Fig. 4-1 Efficacy of E6005 in Japanese adult patients with atopic dermatitis.

Differences in EASI (eczema area and severity index) score were analyzed using a linear mixed-effect model, with treatment and time as factors, baseline score as a covariate, subject as random effect, and changes from baseline as repeated measurements. BL (baseline, day1), D5 (day 5) and D11 (day 11) represent assessment days of severity score. 0.01%, 0.03%, 0.1% and 0.2% represent concentration of E6005 ointment.

Acknowledgements

I would like to express my deep gratitude to all those who provided guidance, support and encouragement during the preparation of this dissertation.

Most of all, I would like to express my sincere thanks to Professor Hideyuki Shigemori (University of Tsukuba) for his valuable guidance and encouragement in this study.

I appreciate Professor Takeo Usui, Associate professor Shigeki Yoshida, and Associate professor Kosumi Yamada (University of Tsukuba) for their precise review and valuable comments to this dissertation.

I also would like to express my gratitude to all collaborators and coworkers for their leading me in the appropriate direction throughout my research work. Especially, I would like to note the invaluable assistance given by Dr. Toshio Imai (KAN Research Institute, Inc.). Without his guidance and persistent help this thesis would not have been possible.

I thank Kazuki Miyazaki, Yasutaka Takase, Ichiro Yoshida, Tadashi Okabe, Yasunobu Matsumoto, Nobuhisa Watanabe, Yoshiaki Ohashi, Yuji Onizawa and Hitoshi Harada (Eisai Co. Ltd.) for synthesizing and providing us with samples of the compounds.

Finally, I appreciate greatly the support of my son, my daughter and my wife.

References

[1] Drews J. Drug discovery: a historical perspective. Science. 2000; 287: 1960-64.

[2] Umezu K. Systematized survey on the history of drug discovery with technical development. Center of the History of Japanese Industrial Technology. 2015; 22: 83-221.

[3] Miyazaki K, Takase Y and Saeki T (1999) inventors, Eisai Co., Ltd. assignee. Nitrogenous heterocyclic derivatives and medicine thereof. WO199937622

[4] Miyazaki K, Kusano K, Takase Y, Asano O, Shirato M, Wakita H, Ishii N ,Saeki T (2007) inventors, Eisai R&D Management Co., Ltd. assignee. 4-(3-benzoylaminophenyl)-6,7-dimethoxy-2-methylaminoquinazoline derivative. WO2007097317

[5] Wakita H, Yanagawa T, Kuboi Y and Imai T. E6130, a novel CX3C chemokine receptor 1 (CX3CR1) modulator, attenuates mucosal inflammation and reduces $CX3CR1^{+}$ leukocyte trafficking in mice with colitis. Mol Pharmacol. 2017; 92: 502-9.

[6] Yoshida I, Okabe T, Matsumoto Y, Watanabe N, Ohashi Y, Onizawa Y and Harada H (2013) inventors, Eisai R&D Management Co., Ltd., assignee. Pyrrolidin-3-ylacetic acid derivative. US Patent 8476301. 2013 Jul 02

[7] Ikoma A, Rukwied R, Ständer S, Steinhoff M, Miyachi Y and Schmelz M. Neuronal sensitization for histamine-induced itch in lesional skin of patients with atopic dermatitis. Arch Dermatol. 2003; 139: 1455-8.

[8] Akiyama T, Carstens MI and Carstens E. Enhanced scratching evoked by PAR-2 agonist and 5-HT but not histamine in a mouse model of chronic dry skin itch. Pain. 2010; 151: 378-83.

[9] Wahlgren CF. Itch and atopic dermatitis: an overview. J Dermatol. 1999; 26: 770-9.

[10] Williams H, Robertson C, Stewart A, Aït-Khaled N, Anabwani G, Anderson R, Asher I, Beasley R, Björkstén B, Burr M, Clayton T, Crane J, Ellwood P, Keil U, Lai C, Mallol J, Martinez F, Mitchell E, Montefort S, Pearce N, Shah J, Sibbald B, Strachan D, von Mutius E and Weiland SK. Worldwide variations in the prevalence of symptoms of atopic eczema in the international study of asthma and allergies in childhood. J Allergy Clin Immunol. 1999; 103: 125-38.

[11] Asher MI, Montefort S, Björkstén B, Lai CK, Strachan DP, Weiland SK and Williams H; ISAAC Phase Three Study Group. Worldwide time trends in the prevalence of symptoms of asthma, allergic rhinoconjunctivitis, and eczema in childhood: ISAAC Phases One and Three repeat multicountry cross-sectional surveys. Lancet. 2006; 368: 733–43.

[12] Muto T, Hsieh SD, Sakurai Y, Yoshinaga H, Suto H, Okumura K and Ogawa H. Prevalence of atopic dermatitis in Japanese adults. Br J Dermatol. 2003; 148: 117–21.

[13] Saeki H. Assessment of usefulness in survey of adult AD prevalence and survey of AD in school children in improvement survey. 2004 Health and Labour Sciences Research Grant, Prevention of immunological allergic diseases /Medical research industry report. 2005; 3: 41-3.

[14] Hanifin JM and Reed ML. A population-based survey of eczema prevalence in the United States. Dermatitis. 2007; 82: 82-91.

[15] Wolff K, Goldsmith LA, Katz SI, Gilchrest BA, Paller AS and Leffell DJ. Atopic Dermatitis (Atopic Eczema). Fitzpatrick's Dermatology in General Medicine, 7th ed. New York: Mcgraw-Hill; 2007.

[16] Tamaki K, general editor. Comprehensive handbook of clinical dermatology. Vol. 3 Eczema, prurigo, pruritus, erythroderma, urticaria. Tokyo: Nakayama Shoten; 2002.

[17] Homey B, Steinhoff M, Ruzicka T and Leung DY. Cytokines and chemokines orchestrate atopic skin inflammation. J Allergy Clin Immunol. 2006; 118: 178-89.

[18] Vestergaard C, Bang K, Gesser B, Yoneyama H, Matsushima K and Larsen CG. A Th2 chemokine, TARC, produced by keratinocytes may recruit $CLA^{+}CCR4^{+}$ lymphocytes into lesional atopic dermatitis skin. J Invest Dermatol. 2000; 115: 640-6.

[19] Bieber T. Atopic dermatitis. N Eng J Med. 2008; 358: 1483-94.

[20] Abrahamsen H, Baillie G, Ngai J, Vang T, Nika K, Ruppelt A, Mustelin T, Zaccolo M, Houslay M and Taskén K. TCR- and CD28-mediated recruitment of phosphodiesterase 4 to lipid rafts potentiates TCR signaling. J Immunol. 2004; 173: 4847-58.

[21] Jin SLC, Lan L, Zoudilova M and Conti M. Specific Role of phosphodiesterase 4B in lipopolysacchride-induced signaling in mouse macrophages. J Immunol. 2005; 175: 1523-31.

[22] Hanifin JM and Chan SC. Monocyte phosphodiesterase abnormalities and dysregulation of lymphocyte function in atopic dermatitis. J Invest Dermatol. 1995; 105: 84S-88S.

[23] Imokawa G, Abe A, Jin K, Higaki Y, Kawashima M and Hidano A. Decreased level of ceramides in stratum corneum of atopic dermatitis: An etiologic factor in atopic dry skin? J Invest Dermatol. 1991; 96: 523-6.

[24] Wahlgren CF. Itch and atopic dermatitis: An overview. J Dermatol. 1999; 26: 770-9.

[25] Ikoma A., Fartasch M., Heyer G., Miyachi Y., Handwerker H. and Schmelz M. Painful stimuli evoke itch in patients with chronic pruritus: Central sensitization for itch. Neurology. 2004; 62: 212-7.

[26] Urashima R and Mihara M. Cutaneous nerves in atopic dermatitis. A histological, immunohisto- chemical and electron microscopic study. Virchows Arch. 1998; 432: 363-70.

[27] Schmelz M, Hilliges M, Schmidt R, Ørstavik K, Vahlquist C, Weidner C, Handwerker HO and Torebjörk HE. Active "itch fibers" in chronic pruritus. Neurology. 2003; 61: 564-6.

[28] Ikoma A, Steinhoff M, Ständer S, Yosipovitch G and Schmelz M. The neurobiology of itch. Nat Rev Neurosci. 2006; 7: 535-47.

[29] Steinhoff M, Bienenstock J, Schmelz M, Maurer M, Wei E and Bíró T. Neurophysiological, neuroimmunological, and neuroendocrine basis of pruritus. J Invest Dermatol. 2006; 126: 1705-18.

[30] Akdis CA, Akdis M, Bieber T, Bindslev-Jensen C, Boguniewicz M, Eigenmann P, Hamid Q, Kapp A, Leung DY, Lipozencic J, Luger TA, Muraro A, Novak N, Platts-Mills TA, Rosenwasser L, Scheynius A, Simons FE, Spergel J, Turjanmaa K, Wahn U, Weidinger S, Werfel T and Zuberbier T; European Academy of Allergology; Clinical Immunology/American Academy of Allergy, Asthma and Immunology/PRACTALL Consensus Group. Diagnosis and treatment of atopic dermatitis in children and adults: European Academy of Allergology and Clinical Immunology/ American Academy of Allergy, Asthma and Immunology/ PRACTALL Consensus Report. J Allergy Clin Immunol. 2006; 118: 152-69.

[31] Furue M, Saeki H, Furukawa F, Hide M, Ohtsuki M, Nakamura T, Sasaki R, Suto H and Takehara K. Guideline for management of atopic dermatitis. Jpn J Dermatol. 2008; 118: 325-42.

[32] Zuberbier T, Orlow S, Paller A, Taïeb A, Allen R, Hernanz-Hermosa J,

Ocampo-Candiani J, Cox M, Langeraar J and Simon JC. Patient perspectives on the management of atopic dermatitis. J Allergy Clin Immunol. 2006; 118: 226-32.

[33] Ishii N, Shirato M, Wakita H, Miyazaki K, Takase Y, Asano O, Kusano K, Yamamoto E, Inoue C and Hishinuma I. Anti-pruritic effect of the topical phosphodiesterase 4 inhibitor E6005 ameliorates skin lesions in a mouse atopic dermatitis model. J Pharmacol Exp Ther. 2013; 346: 105-12.

[34] Dedov VN, Mandadi S, Armati PJ and Verkhratsky A. Capsaicin-induced depolarization of mitochondria in dorsal root ganglion neurons is enhanced by vanilloid receptors. Neuroscience. 2001; 103: 219-26.

[35] Li C, Peoples RW, Lanthorn TH, Li ZW and Weight FF. Distinct ATP-activated currents in different types of neurons dissociated from rat dorsal root ganglion. Neurosci Lett. 1999; 263: 57-60.

[36] Hiura A and Nakagawa H. An overview of the actions of capsaicin and its receptor, trpv1, and their relations to small primary sensory neurons. Antiinflamm Antiallergy Agents Med Chem. 2011; 10: 2-9.

[37] Inagaki N, Igeta K, Kim JF, Nagao M, Shiraishi N, Nakamura N and Nagai H. Involvement of unique mechanisms in the induction of scratching behavior in BALB/c mice by compound 48/80. Eur J Pharmacol. 2002; 448: 175-83.

[38] Tamura T, Amano T, Ohmori K and Manabe H. The effects of olopatadine hydrochloride on the number of scratching induced by repeated application of oxazolone in mice. Eur J Pharmacol. 2005; 524: 149-54.

[39] Monroe EW. Efficacy and safety of nalmefene in patients with severe pruritus caused by chronic urticaria and atopic dermatitis. J Am Acad Dermatol. 1989; 21: 135-6.

[40] Takano N, Arai I, Hashimoto Y and Kurachi M. Evaluation of antipruritic effects of several agents on scratching behavior by NC/Nga mice. Eur J Pharmacol. 2004; 495: 159-65.

[41] Schmelz M, Schmidt R and Bickel A. Specific C-receptors for itch in human skin. J Neurosci. 1997; 17: 8003-8.

[42] Kim SJ, Park GH, Kim D, Lee J, Min H, Wall E, Lee CJ, Simon MI, Lee SJ and Han SK. Analysis of cellular and behavioral responses to imiquimod reveals a unique itch pathway in transient receptor potential vanilloid 1 (TRPV1)-expressing neurons. Proc Natl Acad Sci USA. 2011; 108: 3371-6.

[43] Han L, Ma C, Liu Q, Weng HJ, Cui Y, Tang Z, Kim Y, Nie H, Qu L, Patel KN, Li Z, McNeil B, He S, Guan Y, Xiao B, Lamotte RH and Dong X. A subpopulation of nociceptors specifically linked to itch. Nat Neurosci. 2013; 16: 174-82.

[44] Pereira U, Boulais N, Lebonvallet N, Pennec JP, Dorange G and Misery L. Mechanisms of the sensory effects of tacrolimus on the skin. Br. J. Dermatol. 2010; 163: 70-7.

[45] Andoh T, Yoshida T and Kuraishi Y. Topical E6005, a novel phosphodiesterase 4 inhibitor, attenuates spontaneous itch-related responses in mice with chronic atopy-like dermatitis. Experiment Dermatol. 2014; 23: 359-61.

[46] Liu T and Ji R. New insights into the mechanisms of itch: are pain and itch controlled by distinct mechanisms? Eur J Physiol. 2013; 465: 1671-85.

[47] Baumgart DC and Sandborn WJ. Inflammatory bowel disease: clinical aspects and established and evolving therapies. Lancet. 2007; 369: 1641-57.

[48] Charo IF and Ransohoff RM. The many roles of chemokines and chemokine receptors in inflammation. N Engl J Med. 2006; 354: 610-21.

[49] Thomas S and Baumgart DC. Targeting leukocyte migration and adhesion in Crohn's disease and ulcerative colitis. Inflammopharmacology. 2012; 20: 1-18.

[50] Nishimura M, Muramoto K, Kawano T and Imai T. Chemokine as novel therapeutic targets for inflammatory bowel disease. Ann NY Acad Sci. 2009; 1173: 350-6.

[51] Bazan JF, Bacon KB, Hardiman G, Wang W, Soo K, Rossi D, Greaves DR, Zlotnik A and Schall TJ. A new class of membrane-bound chemokine with a CX3C motif. Nature. 1997; 385: 640-4.

[52] Nishimura M, Umehara H, Nakayama T, Yoneda O, Hieshima K, Kakizaki M, Dohmae N, Yoshie O and Imai T. Dual functions of fractalkine/CX3C ligand 1 in trafficking of perforin^{+}/granzyme B^{+} cytotoxic effector lymphocytes that are defined by CX3CR1 expression. J Immunol. 2002; 168: 6173-80.

[53] Imai T, Hieshima K, Haskell C, Baba M, Nagira M, Nishimura M, Kakizaki M, Takagi S, Nomiyama H, Schall TJ, and Yoshie O. Identification and molecular characterization of fractalkine receptor CX3CR1, which mediates both leukocyte migration and adhesion. Cell. 1997; 91: 521-30.

[54] Yoshie O, Imai T and Nomiyama H. Chemokines in immunity. Adv Immunol. 2001; 78: 57-110.

[55] Brand S, Hofbauer K, Dambacher J, Schnitzler F, Staudinger T, Pfennig S, Seiderer J, Tillack C, Konrad A, Göke B, Ochsenkühn T and Lohse P. Increased expression of the chemokine fractalkine in Crohn's disease and association of the fractalkine receptor T280M polymorphism with a fibrostenosing disease phenotype. Am J Gastroenterol. 2006; 101: 99-106.

[56] Kobayashi T, Okamoto S, Iwakami Y, Nakazawa A, Hisamatsu T, Chinen H,

Kamada N, Imai T, Goto H and Hibi T. Exclusive increase of $CX3CR1^{+}$ $CD28^{-}$ $CD4^{+}$ T cells in inflammatory bowel disease and their recruitment as intraepithelial lymphocytes. Inflamm Bowel Dis. 2007; 13: 837-46.

[57] Sans M, Danese S, de la Motte C, de Souza HS, Rivera-Reyes BM, West GA, Phillips M, Katz JA and Fiocchi C. Enhanced recruitment of $CX3CR1^{+}$ T cells by mucosalendothelial cell-derived fractalkine in inflammatory bowel disease. Gastroenterology. 2007; 132: 139-53.

[58] Bassoni DL, Rabb WJ, Achacoso PL, Loh CY and Wehrman TS. Measurements of β-arrestin recruitment to activated seven transmembrane receptors using enzyme complemention. Methods Mol Biol. 2012; 897: 181-203.

[59] Zhao X, Jones A, Olson KR, Peng K, Wehrman T, Park A, Mallari R, Nebalasca D, Young SW and Xiao SH. A mohogeneous enzyme fragment complementation-based β-arrestin translocation assay for high-throughput screening of G-protein-coupled receptors. J Biomol Screen. 2008; 13: 737-47.

[60] Ostanin DV, Bao J, Koboziev I, Gray L, Robinson-Jackson SA, Kosloski-Davidson M, Price VH and Grisham MB. T cell transfer model of chronic colitis: concepts, considerations, and tricks of the trade. Ann J Physiol Gastrointest Liver Physiol. 2009; 296: G135-46.

[61] Kojima R, Kuroda S, Ohkishi T, Nakamaru K and Hatakeyama S. Oxazolone-induced colitis in BALB/C mice: a new method to evaluate the efficacy of therapeutic agents for ulcerative colitis. J Pharmacol Sci. 2004; 96: 307-13.

[62] Ishiguro K, Ando T, Maeda O, Watanabe O and Goto H. Novel mouse model of colitis characterized by hapten-protein visualization. Biotechniques. 2010; 49: 641-8.

[63] Kostadinova FI, Baba T, Ishida Y, Kondo T, Popivanova BK and Mukaida N.

Crucial involvement of the CX3CR1-CX3CL1 axis in dextran sulfate sodium-mediated acute colitis in mice. J Leukoc Biol. 2010; 88: 133-43.

[64] Niess JH and Adler G. Enteric flora expands gut lamina propria CX3CR1+ dendritic cells supporting inflammatory immune responses under normal and inflammatory conditions. J Immunol. 2010; 184: 2026-37.

[65] Medina-Contreras O, Geem D, Laur O, Williams IR, Lira SA, Nusrat A, Parkos CA and Denning TL. CX3CR1 regulates intestinal macrophage homeostasis, bacterial translocation, and colitogenic Th17 responses in mice. J Clin Invest. 2011; 121: 4787-95.

[66] Kayama H, Ueda Y, Sawa Y, Jeon SG, Ma JS, Okumura R, Kubo A, Ishii M, Okazaki T, Murakami M, Yamamoto M, Yagita H and Takeda K. Intestinal CX3C chemokine receptor 1^{high} ($CX3CR1^{high}$) myeloid cells prevent T-cell-dependent colitis. Proc Natl Acad Sci USA. 2012; 109: 5010-5.

[67] Khan WI, Motomura Y, Wang H, El-Sharkawy RT, Verdu EF, Verma-Gandhu M Rollins BJ and Collins SM. Critical role of MCP-1 in the pathogenesis of experimental colitis in the context of immune and enterochromaffin cells. Am J Physiol Gastrointest Liver Physiol. 2006; 291: G803-11.

[68] Bento AF, Leite DF, Claudino RF, Hara DB, Leal PC and Calixto JB. The selective nonpeptide CXCR2 antagonist SB225002 ameliorates acute experimental colitis in mice. J Leukoc Biol. 2008; 84: 1213-21.

[69] Morimura S, Oka T, Sugaya M and Sato S. CX3CR1 deficiency attenuates imiquimod-induced psoriasis-like skin inflammation with decreased M1 macrophages. J Dermatol Sci. 2016; 82: 175-88.

[70] Nemoto O, Hayashi N, Kitahara Y, Furue M, Hojo S, Nomoto M and Shima S;

Japanese E6005 Study Investigators. Effect of topical phosphodiesterase 4 inhibitor E6005 on Japanese children with atopic dermatitis: Results from a randomized, vehicle-controlled exploratory trial. J Dermatol. 2016; 43: 881-7.

[71] Ohba F, Matsuki S, Imayama S, Matsuguma K, Hojo S, Nomoto M and Akama H. Efficacy of a novel phosphodiesterase inhibitor, E6005, in patients with atopic dermatitis: An investigator-blinded, vehicle-controlled study. J Dermatolg Treat. 2016; 27: 467-72.

List of Publications

A putative antipruritic mechanism of the phosphodiesterase-4 inhibitor E6005 by attenuating capsaicin-induced depolarization of C-fibre nerves.

Hisashi Wakita, Masayoshi Ohkuro, Naoto Ishii, Ieharu Hishinuma and Manabu Shirato

Exp Dermatol. 2015; 24: 215-6.

E6130, a novel CX3C chemokine receptor 1 (CX3CR1) modulator, attenuates mucosal inflammation and reduces $CX3CR1^{+}$ leukocyte trafficking in mice.

Hisashi Wakita, Tatsuya Yanagawa, Yoshikazu Kuboi and Toshio Imai.

Mol Pharmacol. 2017; 92: 502-9.